5. Kuramochi M, Fukuhara H, Nobukuni T, Kanbe T, Maruyama T, et al. (2001) TSLC1 is a tumor-suppressor gene in human non-small-cell lung cancer. Nat Genet 27: 427–430.
6. Murakami Y (2005) Involvement of a cell adhesion molecule, TSLC1/IGSF4, in human oncogenesis. Cancer Sci 96: 543–552.
7. Yageta M, Kuramochi M, Masuda M, Fukami T, Fukuhara H, et al. (2002) Direct association of TSLC1 and DAL-1, two distinct tumor suppressor proteins in lung cancer. Cancer Res 62: 5129–5133.
8. Fukuhara H, Masuda M, Yageta M, Fukami T, Kuramochi M, et al. (2003) Association of a lung tumor suppressor TSLC1 with MPP3, a human homologue of Drosophila tumor suppressor Dlg. Oncogene 22: 6160–6165.
9. Sakurai-Yageta M, Masuda M, Tsuboi Y, Ito A, Murakami Y (2009) Tumor suppressor CADM1 is involved in epithelial cell structure. Biochem Biophys Res Commun 390: 977–982.
10. Shingai T, Ikeda W, Kakunaga S, Morimoto K, Takekuni K, et al. (2003) Implications of nectin-like molecule-2/IGSF4/RA175/SgIGSF/TSLC1/SynCAM1 in cell-cell adhesion and transmembrane protein localization in epithelial cells. J Biol Chem 278: 35421–35427.
11. Biederer T, Sara Y, Mozhayeva M, Atasoy D, Liu X, et al. (2002) SynCAM, a synaptic adhesion molecule that drives synapse assembly. Science 297: 1525–1531.
12. Dimitratos SD, Woods DF, Stathakis DG, Bryant PJ (1999) Signaling pathways are focused at specialized regions of the plasma membrane by scaffolding proteins of the MAGUK family. Bioessays 21: 912–921.
13. Zheng CY, Seabold GK, Horak M, Petralia RS (2011) MAGUKs, synaptic development, and synaptic plasticity. Neuroscientist 17: 493–512.
14. Wang D, You Y, Case SM, McAllister-Lucas LM, Wang L, et al. (2002) A requirement for CARMA1 in TCR-induced NF-kappa B activation. Nat Immunol 3: 830–835.
15. Weiger MC, Wang CC, Krajcovic M, Melvin AT, Rhoden JJ, et al. (2009) Spontaneous phosphoinositide 3-kinase signaling dynamics drive spreading and random migration of fibroblasts. J Cell Sci 122: 313–323.
16. Furuno T, Ito A, Koma Y, Watabe K, Yokozaki H, et al. (2005) The spermatogenic Ig superfamily/synaptic cell adhesion molecule mast-cell adhesion molecule promotes interaction with nerves. J Immunol 174: 6934–6942.
17. Watton SJ, Downward J (1999) Akt/PKB localisation and 3′ phosphoinositide generation at sites of epithelial cell-matrix and cell-cell interaction. Curr Biol 9: 433–436.
18. Qian Y, Corum L, Meng Q, Blenis J, Zheng JZ, et al. (2004) PI3K induced actin filament remodeling through Akt and p70S6K1: implication of essential role in cell migration. Am J Physiol Cell Physiol 286: C153–163.
19. Vivanco I, Sawyers CL (2002) The phosphatidylinositol 3-Kinase AKT pathway in human cancer. Nat Rev Cancer 2: 489–501.
20. Laprise P, Viel A, Rivard N (2004) Human homolog of disc-large is required for adherens junction assembly and differentiation of human intestinal epithelial cells. J Biol Chem 279: 10157–10166.
21. Karnak D, Lee S, Margolis B (2002) Identification of multiple binding partners for the amino-terminal domain of synapse-associated protein 97. J Biol Chem 277: 46730–46735.
22. Boles KS, Barchet W, Diacovo T, Cella M, Colonna M (2005) The tumor suppressor TSLC1/NECL-2 triggers NK-cell and CD8+ T-cell responses through the cell-surface receptor CRTAM. Blood 106: 779–786.
23. Wennstrom S, Hawkins P, Cooke F, Hara K, Yonezawa K, et al. (1994) Activation of phosphoinositide 3-kinase is required for PDGF-stimulated membrane ruffling. Curr Biol 4: 385–393.
24. Gassama-Diagne A, Yu W, ter Beest M, Martin-Belmonte F, Kierbel A, et al. (2006) Phosphatidylinositol-3,4,5-trisphosphate regulates the formation of the basolateral plasma membrane in epithelial cells. Nat Cell Biol 8: 963–970.
25. Jeanes A, Smutny M, Leerberg JM, Yap AS (2009) Phosphatidylinositol 3′-kinase signalling supports cell height in established epithelial monolayers. J Mol Histol 40: 395–405.
26. Kovacs EM, Ali RG, McCormack AJ, Yap AS (2002) E-cadherin homophilic ligation directly signals through Rac and phosphatidylinositol 3-kinase to regulate adhesive contacts. J Biol Chem 277: 6708–6718.
27. Masuda M, Kikuchi S, Maruyama T, Sakurai-Yageta M, Williams YN, et al. (2005) Tumor suppressor in lung cancer (TSLC)1 suppresses epithelial cell scattering and tubulogenesis. J Biol Chem 280: 42164–42171.

Published OnlineFirst October 31, 2013; DOI: 10.1158/0008-5472.CAN-13-0436

Molecular and Cellular Pathobiology

Cancer Research

HTLV-1 bZIP Factor Suppresses Apoptosis by Attenuating the Function of FoxO3a and Altering Its Localization

Azusa Tanaka-Nakanishi, Jun-ichirou Yasunaga, Ken Takai, and Masao Matsuoka

Abstract

As the infectious agent causing human adult T-cell leukemia (ATL), the human T-cell leukemia virus type 1 (HTLV-1) virus spreads *in vivo* primarily by cell-to-cell transmission. However, the factors that determine its transmission efficiency are not fully understood. The viral genome encodes the HTLV-1 bZIP factor (HBZ), which is expressed in all ATL cases and is known to promote T-cell proliferation. In this study, we investigated the hypothesis that HBZ also influences the survival of T cells. Through analyzing the transcriptional profile of HBZ-expressing cells, we learned that HBZ suppressed transcription of the proapoptotic gene *Bim* (*Bcl2l11*) and that HBZ-expressing cells were resistant to activation-induced apoptosis. Mechanistic investigations into how HBZ suppresses *Bim* expression revealed that HBZ perturbs the localization and function of FoxO3a, a critical transcriptional activator of the genes encoding Bim and also Fas ligand (FasL). By interacting with FoxO3a, HBZ not only attenuated DNA binding by FoxO3a but also sequestered the inactive form of FoxO3a in the nucleus. In a similar manner, HBZ also inhibited *FasL* transcription induced by T-cell activation. Further study of ATL cells identified other Bim perturbations by HBZ, including at the level of epigenetic alteration, histone modification in the promoter region of the Bim gene. Collectively, our results indicated that HBZ impairs transcription of the *Bim* and *FasL* genes by disrupting FoxO3a function, broadening understanding of how HBZ acts to promote proliferation of HTLV-1–infected T cells by blocking their apoptosis. *Cancer Res; 74(1); 188–200. ©2013 AACR.*

Introduction

Human T-cell leukemia virus type 1 (HTLV-1) is estimated to infect 10 to 20 million people in the world (1). This virus causes not only a neoplastic disease of $CD4^+$ T cells, adult T-cell leukemia (ATL), but also chronic inflammatory diseases of the central nervous system, lung, or skin (2). HTLV-1 can be transmitted efficiently in a cell-to-cell fashion (3, 4), whereas free virus shows poor infectivity (5, 6), and virions are not detected in infected individuals. To increase the number of infected cells and facilitate transmission, HTLV-1 increases its copy number primarily by triggering the proliferation of infected cells, replicating within the host genome instead of undergoing viral replication (7, 8). Thus, HTLV-1 promotes proliferation and suppresses apoptosis of infected cells via complex interactions of viral proteins with host factors.

Among the viral genes encoded in HTLV-1, the *tax* gene has been extensively studied. Tax can activate various signal pathways like NF-κB, AP-1, and SRF (9). However, Tax expression is frequently undetectable in ATL cases. Importantly, the nonsense mutations in the *tax* gene are often observed in not only ATL cases but also infected cells of asymptomatic HTLV-1 carriers (10). These findings suggest that other mechanisms suppress the apoptosis of HTLV-1–infected cells in the absence of Tax expression (2). We have reported that the *HTLV-1 bZIP factor (HBZ)* gene is expressed in all ATL cases (11). Furthermore, HBZ promotes the proliferation of T cells and induces development of T-cell lymphomas and inflammatory diseases in transgenic mice (12). Therefore, we speculated that HBZ might also influence apoptosis.

There are two major pathways for apoptosis: the extrinsic and intrinsic apoptotic pathways, which are mediated by Fas and Bim, respectively (13). ATL cells are known to express high levels of Fas antigen, and are susceptible to Fas-mediated signaling (14). However, FasL expression is suppressed in ATL cells by silencing of the *early growth response 3* (*EGR3*) gene transcription, a phenomenon that enables ATL cells to escape activation-induced cell death (15). In addition, Tax increases expression of c-FLIP, which confers resistance to Fas-mediated apoptosis (16, 17). Furthermore, activation of NF-κB by Tax also enables HTLV-1–infected cells to be resistant to apoptosis (18). To date, the effects of HTLV-1 infection on Bim-mediated apoptosis remain unknown.

In this study, we analyzed transcriptional changes induced by HBZ expression in T cells, and found that transcription of a proapoptotic gene, *Bim*, was hindered by HBZ. This suppression led to decreased activation-induced cell death. We found that HBZ suppressed *Bim* transcription by targeting FoxO3a, a critical transcription factor for the *Bim* and *FasL* gene. In some

Authors' Affiliation: Laboratory of Virus Control, Institute for Virus Research, Kyoto University, Sakyo-ku, Kyoto, Japan

Note: Supplementary data for this article are available at Cancer Research Online (http://cancerres.aacrjournals.org/).

Corresponding Author: M. Matsuoka, Institute for Virus Research, Kyoto University, 53 Shogoin Kawahara-cho, Sakyo-ku, Kyoto 606-8507, Japan. Phone: 81-757-514-048; Fax: 81-757-514-049; E-mail: mmatsuok@virus.kyoto-u.ac.jp

doi: 10.1158/0008-5472.CAN-13-0436

Published OnlineFirst October 31, 2013; DOI: 10.1158/0008-5472.CAN-13-0436

ATL cell lines and ATL cases, the *Bim* gene transcription was also silenced by epigenetic mechanisms, but this phenomenon seemed to be secondary to HBZ-mediated suppression of transcription. Thus, it is suggested that HBZ suppresses both intrinsic and extrinsic apoptotic pathways and contributes to the proliferation of ATL cells.

Materials and Methods

Cell lines and clinical samples

HTLV-1 immortalized cell lines (MT-4), ATL cell lines (ED, TL-Om1, and MT-1), T-cell lines not infected with HTLV-1 (Jurkat, SupT1, and CCRF-CEM) were cultured in RPMI 1640 medium supplemented with 10% FBS and antibiotics at 37°C under a 5% CO_2 atmosphere. Jurkat cells stably expressing spliced form of HBZ (sHBZ), Jurkat-HBZ, were maintained as described previously (19). To construct CCRF-CEM cells stably expressing HBZ, CEM-HBZ, the coding sequence of HBZ was subcloned into pME18Sneo vector and then the expression vector or its empty vector were transfected into CCRF-CEM cells by using Neon (Invitrogen) according to the manufacturer's instructions. Stable transfectants were selected in G418 (1 mg/mL). 293T cells were cultured in Dulbecco's Modified Eagle Medium supplemented with 10% FBS and antibiotics and when 293FT cells were cultured, 500 μg/mL G418 was added. Fas-blocking antibody was purchased from Alexis.

This study was conducted according to the principles expressed in the Declaration of Helsinki. The study was approved by the Institutional Review Board of Kyoto University (G204). All patients provided written informed consent for the collection of samples and subsequent analysis.

Plasmid constructs

Wild-type form of FoxO3a was generated by PCR amplification using Jurkat cDNA library and constitutively active form of FoxO3a (FoxO3aAAA) was also generated by PCR amplification with mutated primers (20). These PCR fragments were then subcloned into pCMV-Tag2B vector and pIRES-hrGFP-1a (Stratagene). The vectors encoding the myc-His-tagged form of HBZ and its mutants used in this study have been described previously (19, 21). We modified pLKO.1-EGFP vector for delivery of anti-FoxO3 short hairpin RNAs (shRNA) to Jurkat, Jurkat-control, and Jurkat-HBZ. shRNA sequence used was 5′-GCACAACCTGTCCTGCATAG-3′. The 6xDBE-Luc construct that contains six FOXO-binding sites known as DAF-16 binding elements (DBE) was kindly provided by Dr. Furuyama (Kagawa Prefectural University of Health Sciences, Kagawa, Japan) and the backbone of this vector was pGL3-basic (Promega; ref. 22).

Luciferase assay

Jurkat cells were transfected with 0.2 μg/well of luciferase reporter plasmid, 1 ng/well of *Renilla* luciferase control vector (phRL-TK), 0.2 μg/well of FoxO3aAAA expression plasmid or its empty vector, and 0.6 μg/well of HBZ expression plasmid or its empty vector with caspase inhibitor Z-VAD-FMK (MBL). Plasmids were transfected using Neon (Invitrogen) according to the manufacturer's instructions. After 24 hours, cells were collected and luciferase activities were measured using the Dual-Luciferase Reporter Assay (Promega). Relative luciferase activity was calculated as the ratio of firefly to *Renilla* luciferase activity. Three independent experiments, each with triplicate transfections, were performed and typical results are shown.

Microarray analysis

Jurkat-control and Jurkat-HBZ were stimulated with phorbol myristate acetate (PMA; 50 ng/mL) and ionomycin (Io; 1 μg/mL) for 9 hours. After the stimulation, cells were collected and total RNA was isolated using TRIzol Reagent (Invitrogen) according to the manufacturer's instructions. We then digested DNA using deoxyribonuclease I (Invitrogen) and cleaned up RNA using RNeasy Mini Kit (Qiagen) according to the manufacturer's instructions. We then synthesized cDNA and performed microarray processing according to the GeneChip Expression Analysis Technical Manual (Affymetrix). All data were analyzed by using GeneSpring GX (Agilent Technologies). The microarray data related to this article have been submitted to the Gene Expression Omnibus under the accession number GSE48029.

Immunofluorescence analysis

293FT cells were transfected with expression vectors using Lipofectamine LTX (Invitrogen) or TransIT (TaKaRa). Twenty-four hours after transfection, cells were reseeded on the poly-L-lysine–coated glass (Matsunami Glass Ind., Ltd.) or poly-D-lysine (Sigma)–coated glass. Twenty-four hours after the reseeding, cells were fixed with 4% paraformaldehyde for 15 minutes and permeabilized with 0.2% Triton X-100 for 15 minutes, and blocked by incubation in 5% BSA/PBS for 30 minutes. For immunostaining, the cells were incubated with anti-Foxo3a, anti-p-Foxo3a (Cell Signaling Technology), Cy3-conjugated anti-c-Myc (Sigma) or biotinylated anti-FLAG (Sigma) antibodies for 1 hour or in case of observation of endogenous expression, cells were incubated overnight at 4°C. Primary antibodies were visualized by incubating the cells with Alexa-Fluor 488–conjugated goat anti-rabbit immunoglobulin G (IgG) antibody (Invitrogen) or AlexaFluor 488–conjugated streptavidin (Invitrogen). Nuclei were stained and mounted with ProLong Gold antifade reagent with 4′,6-diamidino-2-phenylindole (DAPI; Invitrogen). To concentrate nonadherent cells onto a microscope slide, CytoFuge (StatSpin) was used. Fixation and blocking were performed as described earlier.

Assessment of apoptosis

Apoptotic cells were routinely identified by Annexin V-APC (eBioscience) or phycoerythrin (PE) or fluorescein isothiocyanate (FITC; BioVision) -staining according to the manufacturer's instructions and analyzed with a flow cytometer (BD FACSCanto II; BD Biosciences). Data files were analyzed by using FlowJo software (TreeStar).

Real-time PCR

Total RNA was isolated for the analysis using TRIzol reagent. RNA was treated with DNase I to eliminate the genomic DNA. Reverse transcription was performed using random primer and SuperScript III Reverse Transcriptase (Invitrogen). $CD25^-$ $CD4^+$ cells from healthy donor were obtained by using human

Published OnlineFirst October 31, 2013; DOI: 10.1158/0008-5472.CAN-13-0436

CD4 T Lymphocyte Enrichment kit (BD Pharmingen). Then, cells were stimulated with PMA/Io for 9 hours, RNA was isolated, and reverse transcription was performed as described earlier. cDNA products were analyzed by real-time PCR using the Taqman Universal PCR Master Mix (PE Applied Biosystems) or FastStart Universal SYBR Green Master (Roche) and Applied Biosystems StepOnePlus Real-Time PCR System according to the manufacturer's instructions. Specific primers and Taqman probes for the *Bim* gene, *FasL* gene, and *GAPDH* internal control gene were purchased from Applied Biosystems. Primer sequences for the *HBZ* gene and *GAPDH* gene used for the evaluation of the knockdown efficiency in MT-1 cells have been described previously (11, 23). Primer sequences for the *HBZ* gene used for another experiment to evaluate the HBZ expression in Jurkat-HBZ, MT-1, TL-Oml, and ED cells were 5′-ATGGCGGCCTCAGGGCTGTT-3′ and 5′-GCGGCTTTCCTCTTCTAAGG-3′. Primer sequences for the *FoxO3a* gene used were 5′-ACAAACGGCTCACTCTGTCCCAG-3′ and 5′-AGCTCTTGCCAGTTCCCTCATTCTG-3′. All amplifications were conducted in triplicates. The relative quantification was calculated according to the method described in Applied Biosystems ABI prism 7700 SDS User Bulletin #2.

Chromatin immunoprecipitation analysis

Chromatin immunoprecipitation (ChIP) assay was performed according to the protocol recommended by Millipore. Cells were fixed with 1% formaldehyde for 10 minutes at room temperature, washed twice with ice-cold PBS, treated with SDS-lysis buffer (1% SDS, 50 mmol/L EDTA, and 200 mmol/L Tris-HCl) for 10 minutes on ice and then sonicated. Thereafter, the DNA/protein complexes were immunoprecipitated with antibodies specific for acetylated-Histone H3, acetylated-Histone H4, dimethylated-Histone H3 (Lys4), RNA polymerase II clone CTD4H8 (Millipore), trimethylated-Histone H3 (Lys27), anti-trimethyl-Histone H3 (Lys9) antibodies (Cell Signaling Technology), or normal rabbit IgG (Santa Cruz Biotechnology) overnight at 4°C. Immune complexes were collected with salmon sperm DNA-protein A and G Sepharose slurry, washed, and eluted with freshly prepared elution buffer (1% SDS, 100 mmol/L $NaHCO_3$). Protein-DNA complexes were de-cross-linked at 65°C for 4 hours. DNA was purified and subjected to real-time PCR for quantification of the target fragments. Sequences for the primer set are described previously (24, 25). For the evaluation of binding of FoxO3a to the FOXO-binding sites, 293T cells were transfected with 5 μg of 6xDBE-Luc construct, 5 μg of FoxO3aAAA expression plasmid together with or without 5 μg of HBZ plasmid using TransIT in 10-cm dishes. Anti-FLAG (Sigma) antibody was used for the immunoprecipitation. Primers used were 5′-AGTGCAGGTGCCAGAACATT-3′ and 5′-GCCTTATGCAGTTGCTCTCC-3′, which were constructed inside of the pGL3-basic vector. For the evaluation of the DNA-binding capacity of FoxO3a with or without HBZ, expression vectors for the HA-tagged FoxO3a and Flag-tagged HBZ were transiently cotransfected into 293T cells using the TransIT reagent. Twenty-four hours after the transfection, cells were collected and chromatin immunoprecipitation assay was performed as described earlier. For the immunoprecipitation, anti-HA (Sigma) antibody was used. Primers used for *Bim* gene promoter were 5′-CCACCACTTGATTCTTGCAG-3′ and 5′-TCCAGCGCTAGTCTTCCTTC-3′, which were constructed to contain the FOXO-binding sequence located in intron1. Primers used for *FasL* gene promoter were 5′-ACGATAGCACCACTGCACTCC-3′ and 5′-GGCTGCAAACCAGTGGAAC-3′, which were also constructed to contain the three FOXO-binding sequences.

Individual PCRs were carried out in triplicate to control for PCR variation and mean C_t values were collected. Fold difference of the antibody-bound fraction (IP) versus a fixed amount of input (In) was calculated as

$$\mathrm{IP/In} = 2^{-\Delta\Delta C_t} = 2^{-(C_t(\mathrm{IP}) - C_t(\mathrm{In}))}$$

Then, the fold difference value for a target antibody (t) was subtracted by the nonspecific value derived from mouse or rabbit IgG (t_0):

$$(\mathrm{IP/In})^{t} - (\mathrm{IP/In})^{t_0}$$

Bisulfite genomic sequencing

Sodium bisulfite treatment of genomic DNA was performed as described previously (26). DNA regions were amplified using bisulfite-treated genomic DNA by nested PCR. To amplify promoter region (promoter 1) of *Bim*, primers used in the first PCR were 5′-TTTAGAGGGAGGAGAGTTTAAAG-3′ and 5′-CCCTACAACCCAACTCTAACTA-3′. Primers for the second PCR were 5′-AGGGTATAGTGAGAGCGTAGG-3′ and 5′-CAACTCTAACTAACGACCCC-3′. For promoter, two primers used in the first PCR were 5′-GTGTGATTGTTTTTTGAGGG-3′ and 5′-AAAATACCCCCAAACAAAATAC-3′. Primers for the second PCR were 5′-GCGGATTTAGTTGTAGATTTTG-3′ and 5′-ACTCTTTACCCAAAACAAACTTC-3′. PCR products were purified, cloned into pGEM-T Easy vector (Promega), and sequenced using the ABI PRISM 3130 Genetic Analyzer. For CpG methylation analysis, Web-based bisulfite sequencing analysis tool called QUMA (quantification tool for methylation analysis) was used (27).

Coimmunoprecipitation assay, analysis of the p-FoxO3a localization, and immunoblotting

Expression vectors for the relevant genes were transiently cotransfected into 293T cells using the TransIT reagent. Forty-eight hours later, cells were collected and coimmunoprecipitation assays were performed as described previously (28). For the analysis of the p-FoxO3a localization, nuclear and cytoplasmic proteins were extracted using Nuclear Complex Co-IP Kit (Active Motif). The proteins were subjected to SDS-PAGE analysis followed by immunoblotting with various antibodies. Antibodies used were anti-p-FoxO3a, anti-α-tubulin (Sigma), anti-FLAG, anti-HA (Sigma), and anti-His (Marine Biological Laboratory).

Lentiviral vector construction and transfection of the recombinant lentivirus

Lentiviral vector expressing shRNA against HBZ was constructed and recombinant lentivirus was infected as described previously (11). When more than 90% of cells expressed

Published OnlineFirst October 31, 2013; DOI: 10.1158/0008-5472.CAN-13-0436

enhanced green fluorescent protein (EGFP), the *HBZ* and *Bim* gene expressions were analyzed by real-time PCR.

Results

The *Bim* gene transcription is suppressed in HBZ-expressing Jurkat and CCRF-CEM cells

To determine the effects of HBZ on gene expression, we first performed microarray analysis. Jurkat cells with or without expression of spliced form of HBZ (Jurkat-HBZ and Jurkat-control, respectively) were stimulated with PMA and Io for 9 hours. Gene expression profiles were then analyzed by DNA microarray. Table 1 shows the apoptosis-associated genes that were downregulated or upregulated in stimulated Jurkat-HBZ cells. Transcription of the *Bim* gene was prominently downregulated in HBZ-expressing Jurkat cells. To confirm the effect of HBZ on the *Bim* gene expression, we evaluated *Bim* mRNA levels in Jurkat-control and Jurkat-HBZ cells with or without PMA/Io stimulation using real-time PCR. As reported in the previous studies showing that treatment by PMA/Io or other stimulators induced *Bim* expression (29, 30), the *Bim* mRNA level of stimulated Jurkat-control cells was three-times higher than that of unstimulated cells, but that of Jurkat-HBZ cells did not change after stimulation (Fig. 1A). Similarly, increased *Bim* transcription by stimulation was also inhibited by HBZ in CCRF-CEM cells (Fig. 1A).

HBZ inhibits apoptosis

It has been reported that Bim plays an important role in activation-induced cell death and T-cell homeostasis (31). Because the earlier data demonstrated that HBZ inhibits stimulation-induced *Bim* expression, we next investigated whether HBZ inhibits apoptosis in response to PMA/Io stimulation. To test this, Jurkat-control and Jurkat-HBZ were each incubated with or without PMA/Io for 9 hours, and then apoptosis was measured using Annexin V. The percentages of apoptotic cells in Jurkat-control and Jurkat-HBZ were 40.2% and 15% respectively, indicating that HBZ suppressed activation-induced apoptosis (Fig. 1B). We also treated cells with doxorubicin and found that HBZ slightly inhibited doxorubicin-induced apoptosis (Supplementary Fig. S1). Fas-mediated apoptotic pathway might be involved in antiapoptotic effect by HBZ. To assess the effect of Fas-mediated signaling on the activation-induced apoptosis, cells were also treated with or without Fas-blocking antibody (0.5 μg/mL) 30 minutes before the PMA/Io stimulation. The percentage of apoptotic cells without Fas-blocking antibody in Jurkat-control and Jurkat-HBZ were 36.9% and 22.4%, respectively. When cells were treated with Fas-blocking antibody, the percentage of apoptotic cells reduced and those were 24% and 13.2% in Jurkat-control and Jurkat-HBZ, respectively (Fig. 1C). Thus, Fas-blocking antibody partially inhibited apoptosis in Jurkat-HBZ, which indicates that Fas-mediated signals are also implicated in activation-induced cell death. Indeed, we found that the transcription level of *FasL* was suppressed in stimulated Jurkat-HBZ and CEM-HBZ cells compared with Jurkat-control and CEM-control cells (Fig. 1D), suggesting that downregulation of FasL by HBZ was also associated with inhibition of apoptosis.

Table 1. Apoptosis-associated genes that are upregulated or downregulated by HBZ

Gene	Fold change	Gene ontology
API5	2.18	Antiapoptosis
BCL2L11 (Bim)	−9.93	Induction of apoptosis
CARD11	2.87	Regulation of apoptosis
CASP1	2.97	Apoptosis
CD28	4.60	Positive regulation of antiapoptosis
COP1	9.41	Regulation of apoptosis
DEDD2	2.01	Induction of apoptosis via death domain receptors
DYRK2	2.16	Induction of apoptosis
GZMB	−5.90	Apoptosis
HIPK2	2.19	Induction of apoptosis by intracellular signals
NLRP1	3.08	Induction of apoptosis
PI3KR2	−2.68	Negative regulation of antiapoptosis
PLEKHF1	2.99	Induction of apoptosis
PRDX2	−2.10	Antiapoptosis
PRF1	3.95	Virus-infected cell apoptosis
RFFL	2.20	Apoptosis
SPHK1	−4.26	Antiapoptosis
TNFRSF9	−2.61	Induction of apoptosis
TP53INP1	2.32	Apoptosis
VEGFA	−6.96	Negative regulation of apoptosis

NOTE: The table shows a list of apoptosis-associated genes that were downregulated or upregulated (by more than 2-fold) in stimulated Jurkat-HBZ cells identified by microarray analysis.

Published OnlineFirst October 31, 2013; DOI: 10.1158/0008-5472.CAN-13-0436

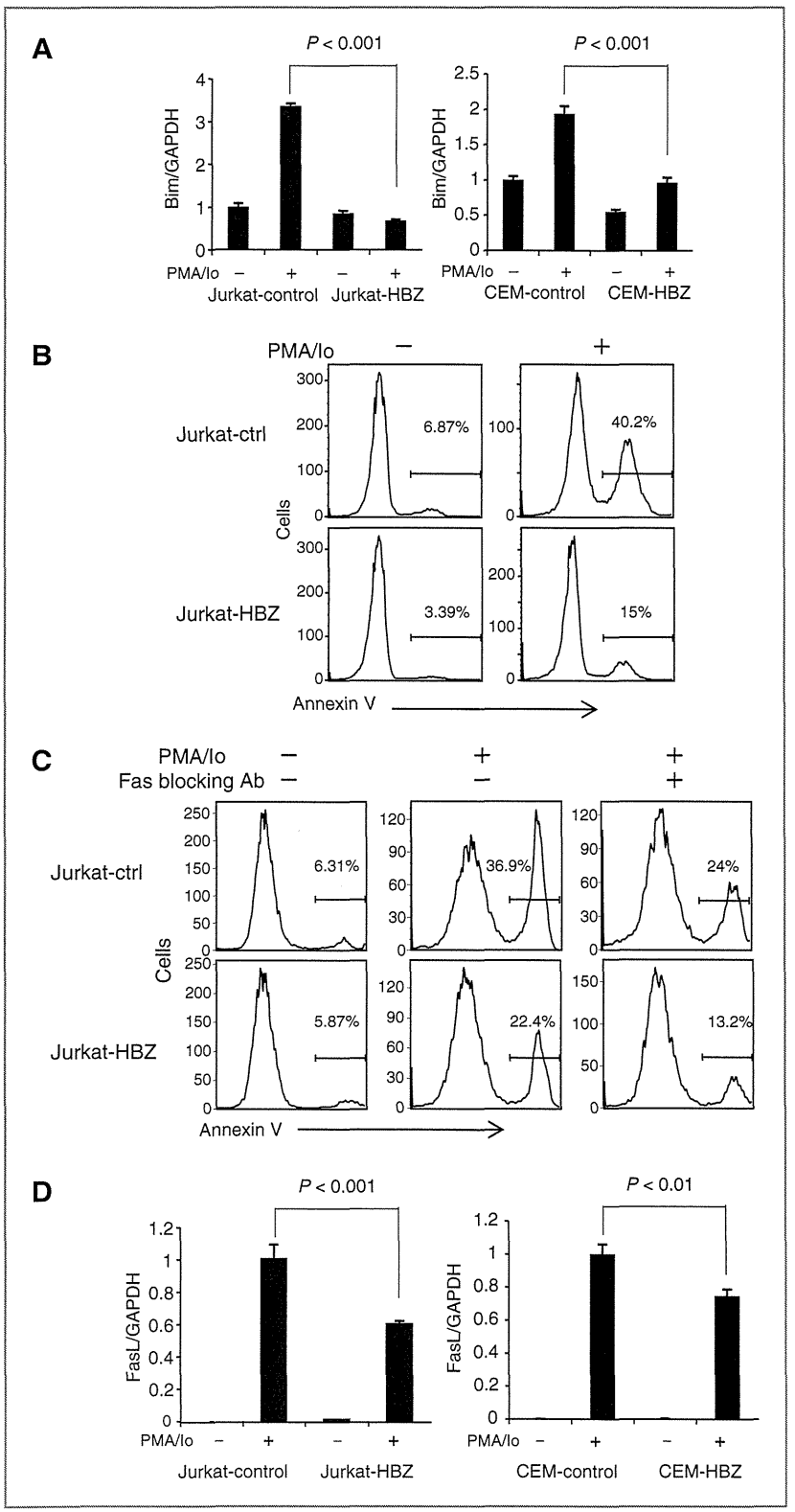

Figure 1. HBZ suppresses the transcription of the *Bim* and *FasL* genes and consequently stimulation-induced apoptosis. A, comparison of the *Bim* mRNA expression in the Jurkat-control, Jurkat-HBZ, CEM-control, and CEM-HBZ cells with or without PMA/Io stimulation by real-time PCR. B, Jurkat-control and Jurkat-HBZ were stimulated with PMA/Io for 9 hours and stained with Annexin V. Percentage of apoptotic cells was determined by flow cytometry. C, Jurkat-control and Jurkat-HBZ were treated with Fas-blocking antibody for 30 minutes and then stimulated with PMA/Io for 9 hours. Percentages of apoptotic cells were monitored by flow cytometry. D, comparison of the *FasL* mRNA transcription in the Jurkat-control, Jurkat-HBZ, CEM-control, and CEM-HBZ cells with or without PMA/Io stimulation by real-time PCR. Error bars, standard deviation. Statistical differences are calculated by Student *t* test. GAPDH, glyceraldehyde-3-phosphate dehydrogenase.

Published OnlineFirst October 31, 2013; DOI: 10.1158/0008-5472.CAN-13-0436

HBZ suppresses *Bim* expression through attenuation of FoxO3a

We analyzed how HBZ suppresses the expression of *Bim* and *FasL*. It has been reported that a forkhead factor, FoxO3a, and p73 are important for the transcription of *Bim* and *FasL* (32, 33). FoxO3a and other FOXO family members are phosphorylated by protein kinases such as Akt or SGK on highly conserved serine and threonine residues (especially Thr32, Ser253, and Ser315 in FoxO3a), resulting in impaired DNA-binding activity and increased binding to the chaperone protein, 14-3-3 (20, 34, 35). Newly formed 14-3-3-FOXO complexes are then exported from the nucleus, thereby inhibiting FOXO-dependent transcription of key target genes such as *Bim*, *FasL*, and *TRAIL* (36).

First, we investigated whether FoxO3a is implicated for the activation induced cell death. As shown in Supplementary Fig. S2, the knockdown of FoxO3a resulted in the decreased apoptotic rate in Jurkat-control cells ($P < 0.05$). Furthermore, inhibition of Foxo3a did not influence activation-induced cell death in Jurkat-HBZ cells, suggesting the inhibitory effect of HBZ on Foxo3a function. To investigate whether HBZ affects FoxO3a function, Jurkat cells were transiently transfected with a plasmid expressing FoxO3aAAA, the constitutive active mutant of FoxO3a, which is no longer phosphorylated by Akt and is localized in the nucleus. The FoxO3aAAA was expressed together with hrGFP using an internal ribosome entry site (IRES; FoxO3aAAA-IREShrGFP). Jurkat cells were transiently transfected with full-length HBZ or its mutants. HBZ has three domains, an activation domain (AD), a central domain (CD), and a basic leucine zipper domain (bZIP; ref. 12). In this study, the deletion mutants (HBZ-ΔAD, HBZ-ΔbZIP, and HBZ-ΔCD) were used. The percentage of FoxO3aAAA induced apoptotic cells in the absence of HBZ was 69.6% while it was suppressed by HBZ (40.6%; $P < 0.001$; Fig. 2A). We also found that an HBZ mutant without activation domain lacks the activity to inhibit FoxO3aAAA-induced apoptosis (Fig. 2A), indicating the significance of activation domain in suppression of FoxO3a-mediated apoptosis. It has been reported that LXXLL motif in FoxO3a binds to its coactivator CBP/p300 (37). Similarly, HBZ has LXXLL-like motifs located in the NH_2-terminal region, which bind to KIX domain of CBP/p300 (38). We speculated that the LXXLL-like motifs of HBZ might affect FoxO3aAAA function through KIX domain of CBP/p300. An HBZ mutant, which has substitutions in 27th and 28th residues (LL to AA) of LXXLL-like motif, lack the activity to suppress FoxO3aAAA-mediated apoptosis (Fig. 2B), indicating that LXXLL-like motif of HBZ is critical for suppression of FoxO3a-mediated apoptosis.

Next, we analyzed the effect of HBZ on a FoxO3a responsive reporter. As shown in Fig. 2C, HBZ suppressed FoxO3a-mediated transcriptional activity ($P < 0.01$). To check whether HBZ inhibits DNA binding of FoxO3a, 293T cells were transiently transfected with FoxO3aAAA and FoxO3a reporter, 6xDBE-Luc, together with or without HBZ. The interaction of FoxO3aAAA to FOXO-binding sites was analyzed by ChIP assay. As shown in Figure 2D, the interaction of FoxO3aAAA to the FOXO-binding sites was interfered by HBZ, suggesting that HBZ inhibits FoxO3a-mediated apoptosis through suppression of the DNA binding of FoxO3a. To clarify the mechanism of HBZ-mediated FoxO3a inhibition, we examined interaction between HBZ and FoxO3a by the immunoprecipitation assay. It showed that HBZ interacted with FoxO3a (Fig. 2E and F). Experiments with FoxO3a deletion mutant revealed that HBZ interacted with the forkhead domain of FoxO3a (Fig. 2E). Analysis using HBZ deletion mutants showed that the central domain of HBZ interacted with FoxO3a (Fig. 2F).

HBZ inhibits nuclear export of phosphorylated form of FoxO3a

Next, we investigated the effect of HBZ on FoxO3a localization by confocal microscopy. We cotransfected 293FT cells with a plasmid expressing human wild-type FoxO3a (FoxO3aWT) protein and an HBZ-expressing plasmid. Consistent with previous reports, FoxO3a remained mainly in cytoplasm when cells were cotransfected with empty vector (Fig. 3A; refs. 20, 34). However, when it was expressed along with HBZ, FoxO3a was localized in both nucleus and cytoplasm (Fig. 3A). To determine whether mislocalized FoxO3a is phosphorylated (pFoxO3a) or not, we used anti-pFoxO3a antibody. Figure 3B and C demonstrated that nuclear-localized FoxO3a was phosphorylated in HBZ-expressing cells. Thereafter, we analyzed the localization of endogenous FoxO3a in HeLa and an ATL cell line, MT-1. Although pFoxO3a was localized widely both in cytoplasm and nucleus in HeLa cells, most pFoxO3a was localized in the nucleus in MT-1 (Fig. 3D), suggesting that endogenous HBZ inhibits the extranuclear translocation of pFoxO3a in this cell line. From the study of crystal structure of the human FoxO3a-DBD/DNA complex, it has been reported that phosphorylation at Ser253 causes a decrease on the DNA-binding ability (39). Abnormal localization of phosphorylated FoxO3a by HBZ might interfere the function of unphosphorylated FoxO3a in the nucleus. The abnormal localization of pFoxO3a prompted us to investigate whether HBZ bound to 14-3-3 along with FoxO3a, as 14-3-3 is a chaperon protein involved in nuclear–cytoplasm shuttling of FOXO family. As shown in Figure 3E, HBZ, FoxO3a, and 14-3-3 form a ternary complex. However, the binding of FoxO3a and 14-3-3 was not affected by HBZ (result of IP with anti-FLAG antibody and detected with anti-HA antibody).

As another possible mechanism for downregulation of *Bim* and *FasL*, we compared the transcription level of *p73* in Jurkat cells with and without HBZ expression. Activation of HBZ-expressing cells reduced transcription of *p73*, but the expression level of *p73* was variable among ATL cell lines (Supplementary Fig. S3A and S3B). We conclude that p73 is not responsible for suppression of *Bim* expression in ATL cells.

Bim expression is suppressed in both ATL cell lines and ATL cases

HBZ has been shown to suppress Bim expression through two different mechanisms as revealed in this study. To analyze Bim expression in ATL cells, we studied *Bim* mRNA levels in non-ATL cell lines and ATL cell lines with or without PMA/Io stimulation, and found that the *Bim* gene transcript was upregulated in Jurkat and CCRF-CEM cells, but not in SupT1 after activation. However, *Bim* transcripts were not increased

Published OnlineFirst October 31, 2013; DOI: 10.1158/0008-5472.CAN-13-0436

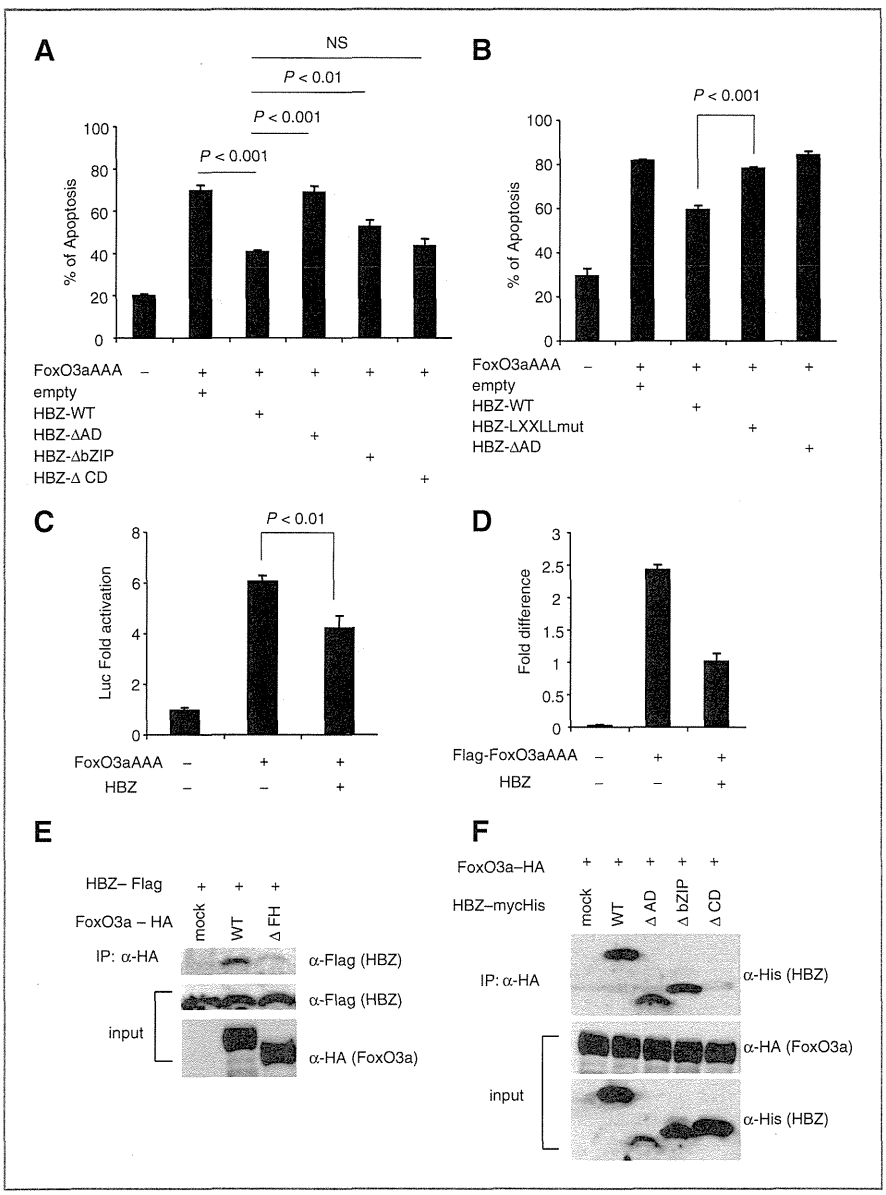

Figure 2. HBZ attenuates function of Foxo3a by physical interaction. A, Jurkat cells were transfected with FoxO3aAAA-expressing vector, a constitutively active form, by using Neon with or without HBZ or its mutants. Twenty-four hours after transfection, cells were stained with Annexin V and analyzed by flow cytometry ($n = 3$). B, Jurkat cells were transfected with FoxO3aAAA-expressing vector together with HBZ or its mutants by using Neon. Cells were stained with Annexin V and analyzed by flow cytometry ($n = 3$). Data are representative of three independent experiments. C, reporter construct containing the 6xDBE and FoxO3aAAA-expressing vector was transiently transfected with or without HBZ into Jurkat cells in the presence of Z-VAD-FMK and luciferase activities were measured. D, 293T cells were transfected with 6xDBE-Luc construct and Flag-tagged FoxO3aAAA expression vector together with or without HBZ expression vector. Cells were immunoprecipitated with anti-FLAG antibody and quantified by real-time PCR. Three independent ChIP experiments were done and representative data are shown. Error bars, experimental variation. E and F, the expression vectors of the indicated proteins were cotransfected into 293T cells, and their interactions were analyzed by immunoprecipitation assay. Data are representative of three independent experiments. Statistical differences are calculated by Student t test.

in all stimulated ATL cell lines (Fig. 4A). The *Bim* gene transcript was also downregulated in primary ATL cells (Fig. 4B) compared with resting peripheral blood mononuclear cells (PBMC) and phytohemagglutinin (PHA)-stimulated T cells. We also stimulated primary ATL cells and normal $CD4^+$ T cells with PMA/Io. The *Bim* gene transcription was quite low in primary ATL sample compared with normal $CD4^+$ T cells even though the cells were stimulated with PMA/Io (Fig. 4C). To confirm HBZ expression in representative ATL cell lines, we quantified the level of the *HBZ* mRNA transcription in Jurkat-HBZ, CEM-HBZ, MT-1, ED, and TL-Om1 by real-time PCR and confirmed that HBZ is expressed in these ATL cell lines (Supplementary Fig. S4). Microarray data, obtained from Gene Expression Omnibus (GEO), show that both *Bim* and *FasL* transcription levels are lower in ATL cases than healthy donors (accession number: GSE33615; Supplementary Fig. S5), supporting our data that *Bim* expression was suppressed in ATL cells.

Bim expression is silenced by epigenetic mechanisms

Because the *Bim* gene transcription was severely suppressed in ATL cells, we investigated the epigenetic status (DNA methylation and histone modification) of the promoter region of the *Bim* gene in ATL cells. A previous study showed that the 0.8 kb region immediately upstream of exon 1 contains the important elements for the control of *Bim* expression

Published OnlineFirst October 31, 2013; DOI: 10.1158/0008-5472.CAN-13-0436

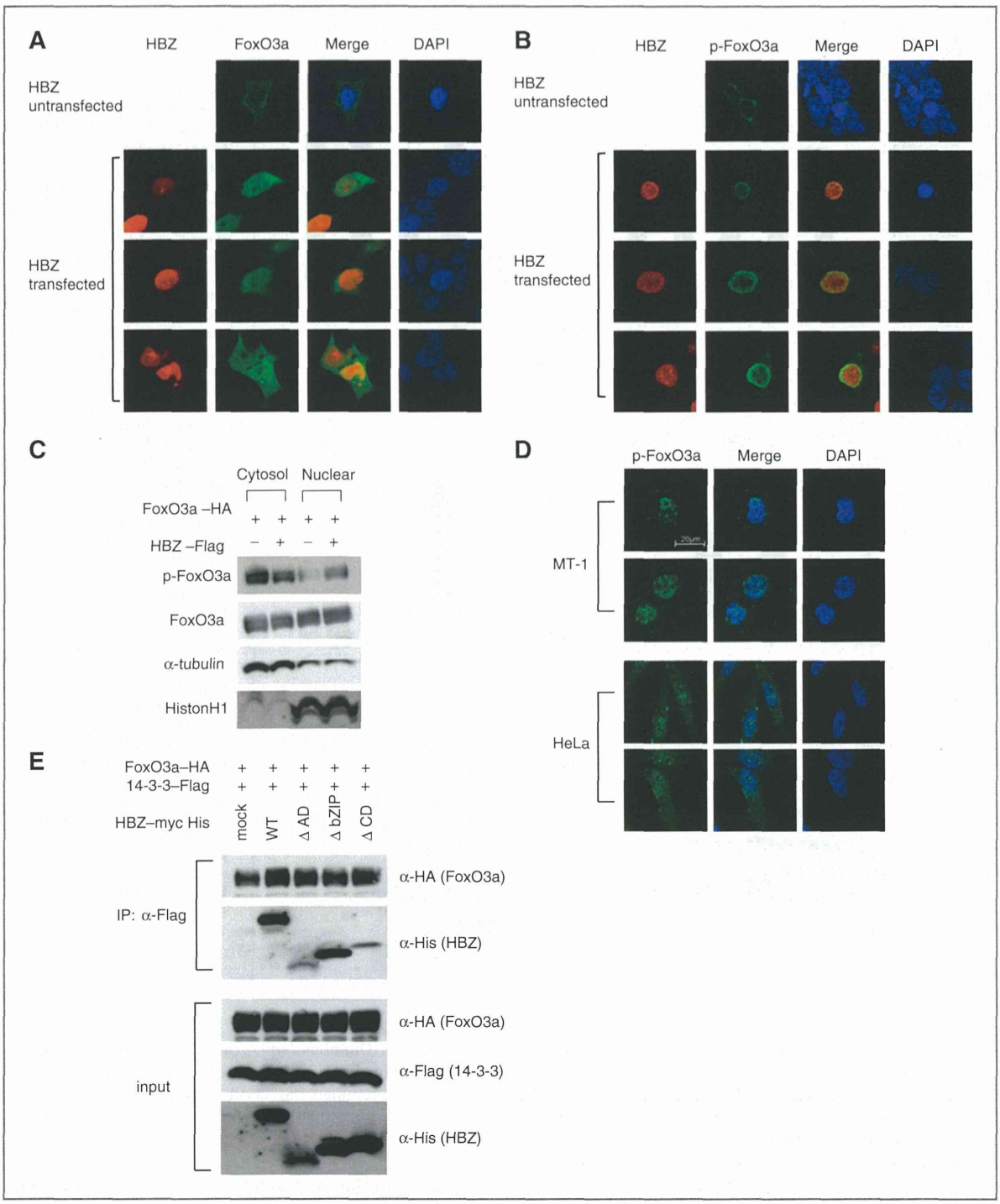

Figure 3. HBZ interferes with normal localization of FoxO3a by forming a ternary complex with FoxO3a and 14-3-3. 293FT cells were transfected with FoxO3aWT-Flag together with or without mycHis-HBZ. A and B, FoxO3a was detected using anti-FLAG-biotin and secondary Streptavidin-Alexa 488 (A), and p-FoxO3a was detected using anti-p-FoxO3a (ser253) and secondary anti-rabbit IgG-Alexa 488 antibody (B). DAPI was used to counterstain the nucleus. C, 293FT cells were transfected with HA-tagged FoxO3aWT together with or without Flag-tagged HBZ. Cytoplasmatic and nuclear fractions were extracted and p-FoxO3a was detected by Western-blotting. D, endogenous localizations of p-FoxO3a (ser253) in HeLa and MT-1 cells were examined using anti-p-FoxO3a. E, the interactions among HBZ, FoxO3a, and 14-3-3 were analyzed by immunoprecipitation.

Published OnlineFirst October 31, 2013; DOI: 10.1158/0008-5472.CAN-13-0436

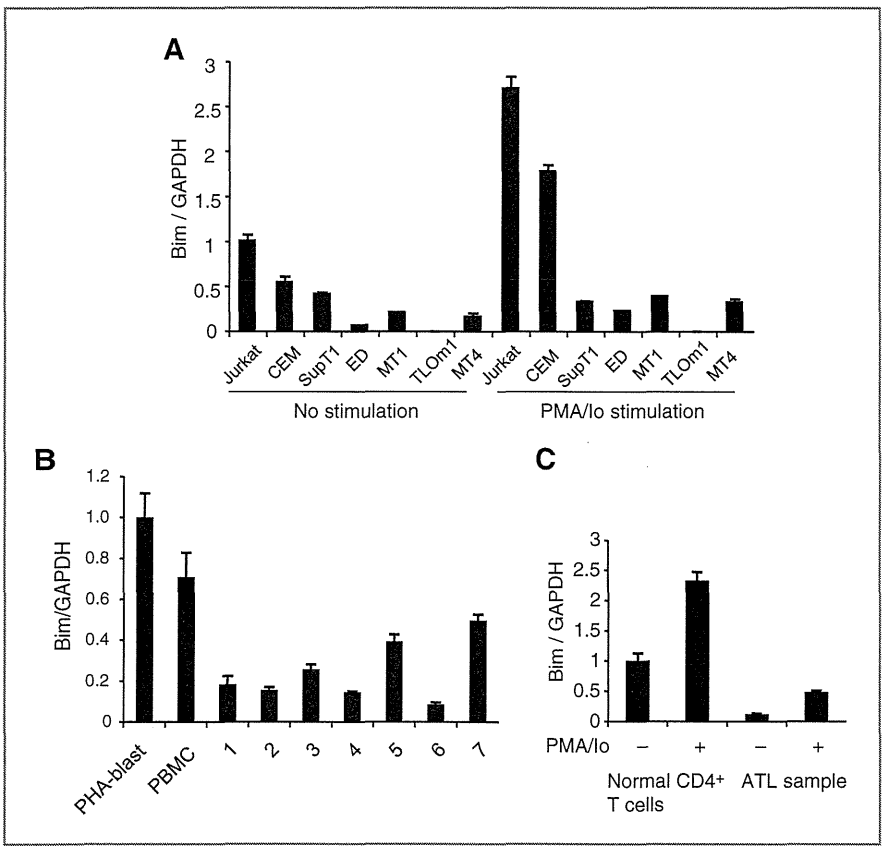

Figure 4. Bim expression is also suppressed in ATL cell lines and ATL cases. Comparison of the *Bim* mRNA expression in non-ATL cell lines and ATL cell lines with or without PMA/Io stimulation (A) and in PBMCs and PHA-blasts from healthy donor samples and fresh ATL samples (B) by real-time PCR. C, comparison of the *Bim* mRNA expression in healthy donor sample and ATL fresh sample with or without PMA/Io stimulation.

(promoter 1). The *Bim* promoter does not contain a TATA or CAAT box and has the characteristics of a "TATA-less" promoter (40). In addition, the alternative promoter has been reported to exist in intron 1 (promoter 2; refs. 41, 42). These two promoter regions are highly GC-rich and contain the binding sites for several transcription factors, including FoxO3a. To determine whether CpG sites in these *Bim* gene promoter regions are methylated in ATL cell lines, their methylation status was analyzed by bisulfite-mediated methylcytosine mapping (Supplementary Fig. S6A and S6B). The promoter 1 of *Bim* was hypermethylated in two ATL cell lines (ED and TL-Om1) and ATL case 1, whereas this region was not so methylated in MT-1 cells and two ATL cases. On the other hand, the promoter 2 was heavily methylated in two ATL cell lines (TL-Om1 and MT-1) and ATL case 1 and partially methylated in Jurkat cells (Supplementary Fig. S6B). These results suggest that in some cases, heavily methylated CpG sites of promoter 1 and 2 are associated with silencing of *Bim* transcription but these methylations can not account for suppressed *Bim* expression in all ATL cell lines and ATL cases.

Therefore, we next focused on the histone modification in the promoter region of *Bim*. It is well known that deacetylation of the histones are also common features of cancer, which results in transcriptional silencing of tumor suppressor genes (43). First, we analyzed the histone H3 and H4 acetylation and H3K4 trimethylation, which are all permissive marks (44), in promoter 1 of Jurkat, MT-1, and TL-Om1 cells. Contrary to our speculation, neither H3, H4 acetylation, nor H3K4 trimethylation differed between MT-1 and Jurkat cells (Supplementary Fig. S7). We next analyzed the histone modification status in promoter 2. As shown in Figure 5A, MT-1 and TL-Om1 cells exhibited decreased level of histone H3 acetylation and H3K4 trimethylation but not histone H4 acetylation. Because methylation of DNA is often preceded by dimethylation of H3K9 or trimethylation of H3K27 (both repressive marks) in oncogenesis (44), we asked whether there were differences in these epigenetic chromatin marks on the *Bim* gene promoter in ATL cell lines. TL-Om1 cells exhibited upregulated level of H3K9 dimethylation and H3K27 trimethylation compared with Jurkat cells (Fig. 5B and C), whereas MT-1 exhibited a little upregulated level of H3K27 trimethylation (Fig. 5C) in the promoter 2. These data suggest that histone modifications of promoter 2 are critical for the suppressed *Bim* gene transcription. We also performed ChIP analysis using anti-RNA polymerase II antibody (Fig. 5D) and revealed that Pol II binding was decreased in MT-1 and TL-Om1 cells, confirming suppressed transcription of the *Bim* gene. To further investigate the mechanisms involved in FoxO3a-mediated *Bim* gene transcription in the promoter 2, we transfected HA-tagged FoxO3a expression vector together with or without a HBZ expression vector into 293T cells and immunoprecipitated with anti-HA antibody. Then, the DNA-binding capacity of FoxO3a was

Published OnlineFirst October 31, 2013; DOI: 10.1158/0008-5472.CAN-13-0436

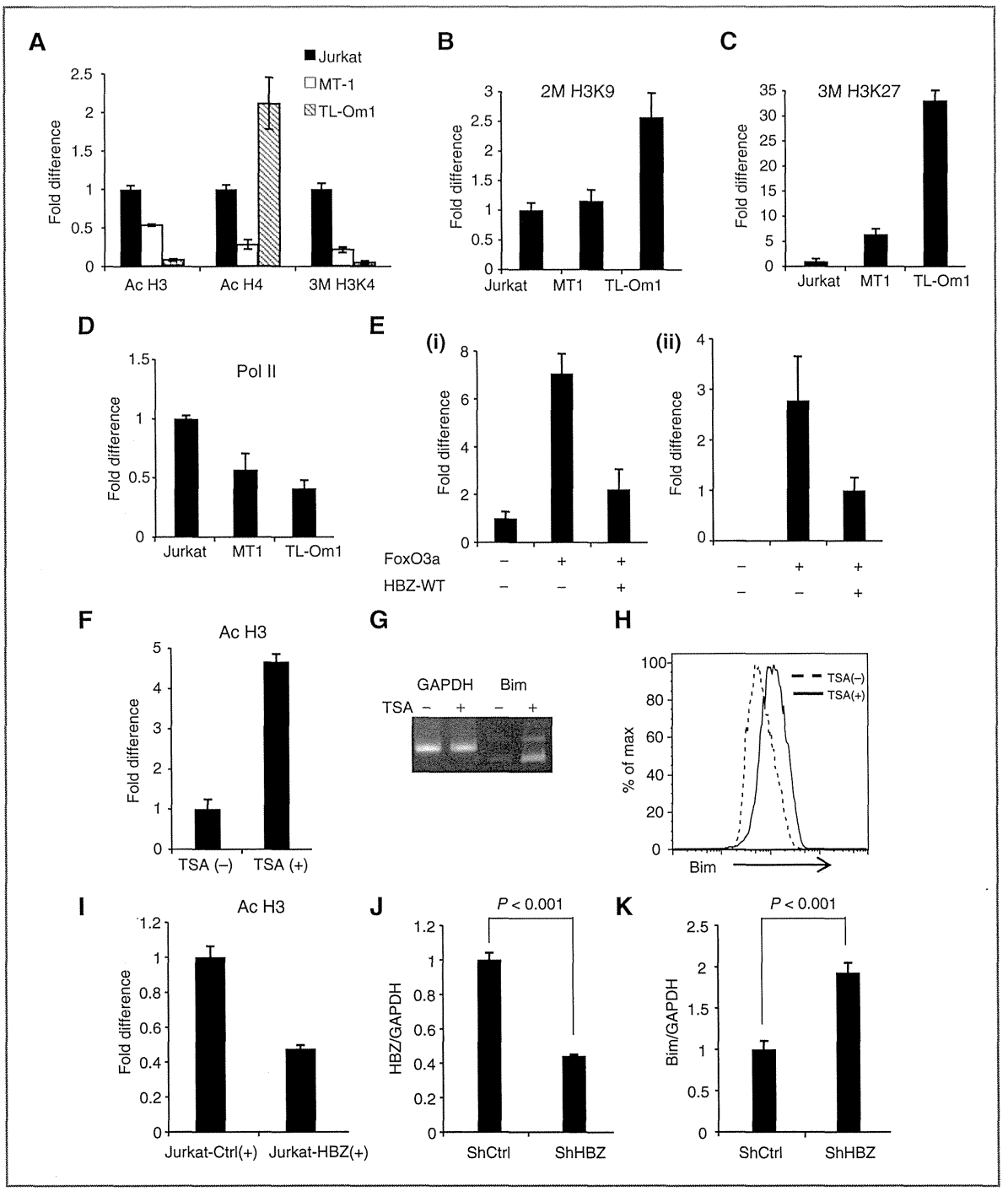

Figure 5. Epigenetic status of the promoter regions of the *Bim* gene. A–C, fold difference of acetylated histone H3, acetylated histone H4, trimethylated H3K4, dimethylated H3K9, or trimethylated H3K27; the data from Jurkat cells were arbitrarily set as 1.0. D, quantitative ChIP assay using RNA polymerase II (Pol II) antibody in Jurkat, MT-1, and TL-Om1 cells. E, 293T cells were transfected with HA-tagged FoxO3a expression vector together with or without HBZ expression vector. Cells were immunoprecipitated with anti-HA antibody and DNA-binding ability at promoter 2 was quantified by real-time PCR. F, fold difference of acetylated histone H3 in MT-1 cells, which were treated with or without 0.4 mmol/L TSA for 15 hours. The data from MT-1 cells without TSA treatment were arbitrarily set as 1.0. G and H, MT-1 cells were treated with 0.4 mmol/L TSA for 15 hours and *Bim* expression level was analyzed by quantitative real-time PCR and flow cytometry. I, fold difference of acetylated histone H3 in the Bim promoter in the Jurkat-control and Jurkat-HBZ cells 9 hours after the stimulation with PMA/Io. J, HBZ transcript in shRNA transfectant of MT-1 was quantified by real-time PCR. K, comparison of the *Bim* mRNA expression in control MT-1 cells and HBZ-KD MT-1 cells. Error bars, experimental variation. The data shown are representative of two or three independent experiments. Statistical differences are calculated by Student *t* test. GAPDH, glyceraldehyde-3-phosphate dehydrogenase.

Published OnlineFirst October 31, 2013; DOI: 10.1158/0008-5472.CAN-13-0436

quantified by real-time PCR. Figure 5E shows that HBZ attenuated the DNA-binding capacity of FoxO3a in the promoter 2 of *Bim* (i) and *FasL* promoter (ii), suggesting that the suppressed binding of FoxO3a to the promoter regions leads to inhibition of the *Bim* and *FasL* genes transcription by HBZ.

Next, we treated MT-1 cells with trichostatin A (TSA), a cell-permeable chemical inhibitor of class I/II histone deacetylases (HDAC). Treatment of TSA resulted in a clear upregulation of acetylation of histone H3 (Fig. 5F) followed by Bim expression both at the mRNA (Fig. 5G) and protein levels (Fig. 5H), indicating that histone modification is associated with suppressed *Bim* transcription in MT-1. We also performed ChIP assay using Jurkat-control and Jurkat-HBZ cells, which were stimulated with PMA and ionomycin for 9 hours, and found that acetylation of histone H3 decreased in Jurkat-HBZ cells (Fig. 5I), suggesting that HBZ is implicated in histone deacetylation in T cells. To verify whether HBZ inhibits transcription of the *Bim* gene, we suppressed the *HBZ* gene transcription by shRNA as reported previously (11). Efficiencies of lentivirus vector transduction, which were determined by EGFP expression, were 90.5% and 90.3% for control MT-1 cells and HBZ-knockdown MT-1 cells, respectively. Suppressed HBZ expression led to increase the *Bim* gene transcription (Fig. 5J and K), indicating that HBZ expression is linked to suppression of *Bim* expression in ATL cells.

Discussion

Human immunodeficiency virus type 1 (HIV-1) replicates vigorously and the generated virus infects target cells *in vivo*. Unlike HIV-1, HTLV-1 induces proliferation to increase the number of infected cells, as this virus is transmitted primarily by cell-to-cell contact (5). Therefore, HTLV-1–encoded proteins promote proliferation of infected cells and inhibit their apoptosis, resulting in an increased number of infected cells *in vivo* (2). In this study, we show that HBZ inhibits both the intrinsic and extrinsic apoptotic pathways via targeting FoxO3a, which leads to suppressed transcriptions of *Bim* and *FasL*. We demonstrated two mechanisms for perturbation of FoxO3a by HBZ: interaction of HBZ with FoxO3a and interference of nuclear export of phosphorylated FoxO3a. HBZ suppresses DNA-binding ability of active form of FoxO3a through interaction between central domain of HBZ and forkhead domain of FoxO3a. In addition, LXXLL-like motif of HBZ is implicated in inhibition of FoxO3a-mediated apoptosis, suggesting that HBZ interferes in interaction of CBP/p300 and FoxO3a. Furthermore, HBZ retains inactive form of FoxO3a in the nucleus through interaction with 14-3-3, leading to transcriptional repression of the target genes. Interestingly, accumulation of phosphorylated form of FoxO3a in the nucleus has been observed in HIV Vpr-expressing cells, which might be implicated in HIV-mediated resistance against insulin (28). Thus, FoxO3a is a target of both human retroviruses.

In this study, we showed that central domain of HBZ interacts with FoxO3a while LXXLL-like motif in activation domain of HBZ is responsible for suppressed apoptosis. LXXLL-like motif of HBZ has been reported to interact with KIX domain of p300 (38). The central domain of HBZ interacts with the forkhead domain of FoxO3a, which binds to the target sequence (35). This is the mechanism how HBZ inhibits DNA binding of FoxO3a. However, inhibitory effect of HBZ on apoptosis largely depends on LXXLL-like motif of activation domain (Fig. 2A and B). FoxO3a is also reported to interact with KIX domain of CBP/p300 (37). Forkhead domain of FoxO3a intramolecularly interacts with its conserved regions (CR) 3, and binding of forkhead domain to DNA releases CR3, allowing it to bind KIX of CBP/p300 (45). These findings suggest that HBZ interferes in the complex interaction between FoxO3a and CBP/p300, which is likely important to induce apoptosis.

It has been reported that Bim has a tumor-suppressor function in various cancers. Hemizygous loss of the *Bim* gene promoted development of B-cell leukemia in Myc-transgenic mice in which c-myc expression was driven by the immunoglobulin gene intron-enhancer (46). Insulin-like growth factor 1 (IGF-1), an important growth factor for myeloma cells, has been reported to suppress Bim expression by epigenetic and posttranslational mechanisms (25). In Epstein–Barr virus–infected B cells, *Bim* transcription is silenced by DNA methylation of the *Bim* gene promoter (47). Thus, impaired expression of Bim is associated with the various cancers, including the virus-related malignancies. FoxO3a is also a target of oncogenesis. BCR-ABL induces phosphorylation of FoxO3a, which leads to suppressed expression of Bim in $Ph1^+$ chronic myelogenous leukemia cells (32). In breast cancer, IκB kinase interacts with, phosphorylates FoxO3a, which causes proteolysis of FoxO3a (48). In this study, we revealed that HBZ hinders nuclear export of phosphorylated FoxO3a, and impairs function of FoxO3a likely through interaction of FoxO3a and p300. Thus, suppressed Bim and FasL expression through inhibition of FoxO3a by HBZ is a new mechanism for oncogenesis.

Besides FoxO3a perturbation by HBZ, we also have identified the epigenetic aberrations in the promoter region of the *Bim* gene in ATL cells, and found that Bim expression is suppressed by DNA methylation and histone modification. ATL cell lines exhibited upregulated level of H3K27 trimethylation in the promoter regions of *Bim*. It has been reported that enhancer of zeste (EZH) 2, a methyltransferase and component of the polycomb repressive complex 2, expression is increased in ATL cell lines (42). Because EZH2 plays an essential role in the epigenetic maintenance of H3K27 trimethylation, upregulated H3K27 trimethylation of the *Bim* gene promoter might be associated with increased expression of EZH2 in ATL cells. In addition, HBZ seems to be associated with histone deacetylation in MT-1 cells. According to the previous studies, it is known that both HBZ and FoxO3a bind to the histone acetyltransferase p300/CBP through the LXXLL motif (38). In this study, we found that the same motif is important for FoxO3a suppression and resulting inhibition of apoptosis. It is likely that HBZ decreases histone acetylation level on Bim promoter through the interaction with FoxO3a and dissociation of p300/CBP from the promoter. In addition to histone modifications, hypermethylation of CpGs in Bim promoter was observed in some ATL cells. These epigenetic aberrations likely occur as the secondary changes following long-time silencing of *Bim* by HBZ, although further investigations will be required.

Published OnlineFirst October 31, 2013; DOI: 10.1158/0008-5472.CAN-13-0436

In this study, we demonstrated that HBZ suppresses activation-induced apoptosis by downregulation of proapoptotic genes, *Bim* and *FasL*. HBZ perturbs the function of FoxO3a by interaction, and induces epigenetic aberrations in the promoter region of the *Bim* gene. It has been shown that HBZ induces not only cancer but also inflammation *in vivo*. Because inflammatory diseases are essentially caused by failure to negatively regulate unnecessary immune responses by apoptosis, suppression of apoptosis by HBZ might be associated with HTLV-1–induced inflammation as well. Collectively, HBZ-mediated inhibition of apoptosis is likely implicated in both neoplastic and inflammatory diseases caused by HTLV-1.

Disclosure of Potential Conflicts of Interest

No potential conflicts of interest were disclosed.

Authors' Contributions

Conception and design: A. Tanaka-Nakanishi, J. Yasunaga, M. Matsuoka
Development of methodology: A. Tanaka-Nakanishi, M. Matsuoka
Acquisition of data (provided animals, acquired and managed patients, provided facilities, etc.): A. Tanaka-Nakanishi, K. Takai
Analysis and interpretation of data (e.g., statistical analysis, biostatistics, computational analysis): A. Tanaka-Nakanishi, J. Yasunaga, K. Takai, M. Matsuoka
Writing, review, and/or revision of the manuscript: A. Tanaka-Nakanishi, J. Yasunaga, M. Matsuoka
Administrative, technical, or material support (i.e., reporting or organizing data, constructing databases): M. Matsuoka
Study supervision: M. Matsuoka

Acknowledgments

The authors thank T. Furuyama (Kagawa Prefectural University of Health Science) for the 6xDBE-Luc plasmid DNA, P. Bouillet for valuable comments on this study, and L. Kingsbury for proofreading of this manuscript.

Grant Support

This study was supported by a Grant-in-aid for Scientific Research from the Ministry of Education, Science, Sports, and Culture of Japan to M. Matsuoka (MEXT grant number 221S0001), a grant from Japan Leukemia Research Fund to M. Matsuoka, and a grant from the Takeda Science Foundation to J. Yasunaga.

The costs of publication of this article were defrayed in part by the payment of page charges. This article must therefore be hereby marked *advertisement* in accordance with 18 U.S.C. Section 1734 solely to indicate this fact.

Received February 14, 2013; revised September 12, 2013; accepted October 5, 2013; published OnlineFirst October 31, 2013.

References

1. Proietti FA, Carneiro-Proietti AB, Catalan-Soares BC, Murphy EL. Global epidemiology of HTLV-I infection and associated diseases. Oncogene 2005;24:6058–68.
2. Matsuoka M, Jeang KT. Human T-cell leukaemia virus type 1 (HTLV-1) infectivity and cellular transformation. Nat Rev Cancer 2007;7:270–80.
3. Igakura T, Stinchcombe JC, Goon PK, Taylor GP, Weber JN, Griffiths GM, et al. Spread of HTLV-I between lymphocytes by virus-induced polarization of the cytoskeleton. Science 2003;299:1713–6.
4. Pais-Correia AM, Sachse M, Guadagnini S, Robbiati V, Lasserre R, Gessain A, et al. Biofilm-like extracellular viral assemblies mediate HTLV-1 cell-to-cell transmission at virological synapses. Nat Med 2010;16:83–9.
5. Derse D, Hill SA, Lloyd PA, Chung H, Morse BA. Examining human T-lymphotropic virus type 1 infection and replication by cell-free infection with recombinant virus vectors. J Virol 2001;75:8461–8.
6. Mazurov D, Ilinskaya A, Heidecker G, Lloyd P, Derse D. Quantitative comparison of HTLV-1 and HIV-1 cell-to-cell infection with new replication dependent vectors. PLoS Pathog 2010;6:e1000788.
7. Cavrois M, Leclercq I, Gout O, Gessain A, Wain-Hobson S, Wattel E. Persistent oligoclonal expansion of human T-cell leukemia virus type 1-infected circulating cells in patients with Tropical spastic paraparesis/HTLV-1 associated myelopathy. Oncogene 1998;17:77–82.
8. Etoh K, Tamiya S, Yamaguchi K, Okayama A, Tsubouchi H, Ideta T, et al. Persistent clonal proliferation of human T-lymphotropic virus type I-infected cells *in vivo*. Cancer Res 1997;57:4862–7.
9. Grassmann R, Aboud M, Jeang KT. Molecular mechanisms of cellular transformation by HTLV-1 Tax. Oncogene 2005;24:5976–85.
10. Fan J, Ma G, Nosaka K, Tanabe J, Satou Y, Koito A, et al. APOBEC3G generates nonsense mutations in HTLV-1 proviral genomes *in vivo*. J Virol 2010;84:7278–87.
11. Satou Y, Yasunaga J, Yoshida M, Matsuoka M. HTLV-I basic leucine zipper factor gene mRNA supports proliferation of adult T cell leukemia cells. Proc Natl Acad Sci U S A 2006;103:720–5.
12. Satou Y, Yasunaga J, Zhao T, Yoshida M, Miyazato P, Takai K, et al. HTLV-1 bZIP factor induces T-cell lymphoma and systemic inflammation *in vivo*. PLoS Pathog 2011;7:e1001274.
13. Bouillet P, O'Reilly LA. CD95, BIM and T cell homeostasis. Nat Rev Immunol 2009;9:514–9.
14. Debatin KM, Goldman CK, Waldmann TA, Krammer PH. APO-1-induced apoptosis of leukemia cells from patients with adult T-cell leukemia. Blood 1993;81:2972–7.
15. Yasunaga J, Taniguchi Y, Nosaka K, Yoshida M, Satou Y, Sakai T, et al. Identification of aberrantly methylated genes in association with adult T-cell leukemia. Cancer Res 2004;64:6002–9.
16. Krueger A, Fas SC, Giaisi M, Bleumink M, Merling A, Stumpf C, et al. HTLV-1 Tax protects against CD95-mediated apoptosis by induction of the cellular FLICE-inhibitory protein (c-FLIP). Blood 2006;107:3933–9.
17. Okamoto K, Fujisawa J, Reth M, Yonehara S. Human T-cell leukemia virus type-I oncoprotein Tax inhibits Fas-mediated apoptosis by inducing cellular FLIP through activation of NF-kappaB. Genes Cells 2006;11:177–91.
18. Sun SC, Yamaoka S. Activation of NF-kappaB by HTLV-I and implications for cell transformation. Oncogene 2005;24:5952–64.
19. Zhao T, Yasunaga J, Satou Y, Nakao M, Takahashi M, Fujii M, et al. Human T-cell leukemia virus type 1 bZIP factor selectively suppresses the classical pathway of NF-kappaB. Blood 2009;113:2755–64.
20. Brunet A, Bonni A, Zigmond MJ, Lin MZ, Juo P, Hu LS, et al. Akt promotes cell survival by phosphorylating and inhibiting a Forkhead transcription factor. Cell 1999;96:857–68.
21. Zhao T, Satou Y, Sugata K, Miyazato P, Green PL, Imamura T, et al. HTLV-1 bZIP factor enhances TGF-{beta} signaling through p300 coactivator. Blood 2011;118:1865–76.
22. Furuyama T, Nakazawa T, Nakano I, Mori N. Identification of the differential distribution patterns of mRNAs and consensus binding sequences for mouse DAF-16 homologues. Biochem J 2000;349:629–34.
23. Ponchel F, Toomes C, Bransfield K, Leong FT, Douglas SH, Field SL, et al. Real-time PCR based on SYBR-Green I fluorescence: an alternative to the TaqMan assay for a relative quantification of gene rearrangements, gene amplifications and micro gene deletions. BMC Biotechnol 2003;3:18.
24. Richter-Larrea JA, Robles EF, Fresquet V, Beltran E, Rullan AJ, Agirre X, et al. Reversion of epigenetically mediated BIM silencing overcomes chemoresistance in Burkitt lymphoma. Blood 2010;116:2531–42.
25. De Bruyne E, Bos TJ, Schuit F, Van Valckenborgh E, Menu E, Thorrez L, et al. IGF-1 suppresses Bim expression in multiple myeloma via epigenetic and posttranslational mechanisms. Blood 2010;115:2430–40.
26. Fan J, Kodama E, Koh Y, Nakao M, Matsuoka M. Halogenated thymidine analogues restore the expression of silenced genes without demethylation. Cancer Res 2005;65:6927–33.

Published OnlineFirst October 31, 2013; DOI: 10.1158/0008-5472.CAN-13-0436

27. Kumaki Y, Oda M, Okano M. QUMA: quantification tool for methylation analysis. Nucleic Acids Res 2008;36:W170–5.
28. Kino T, De Martino MU, Charmandari E, Ichijo T, Outas T, Chrousos GP. HIV-1 accessory protein Vpr inhibits the effect of insulin on the Foxo subfamily of forkhead transcription factors by interfering with their binding to 14-3-3 proteins: potential clinical implications regarding the insulin resistance of HIV-1-infected patients. Diabetes 2005;54:23–31.
29. Cante-Barrett K, Gallo EM, Winslow MM, Crabtree GR. Thymocyte negative selection is mediated by protein kinase C- and Ca2+-dependent transcriptional induction of bim [corrected]. J Immunol 2006;176:2299–306.
30. Snow AL, Oliveira JB, Zheng L, Dale JK, Fleisher TA, Lenardo MJ. Critical role for BIM in T cell receptor restimulation-induced death. Biol Direct 2008;3:34.
31. Green DR, Droin N, Pinkoski M. Activation-induced cell death in T cells. Immunol Rev 2003;193:70–81.
32. Essafi A, Fernandez de Mattos S, Hassen YA, Soeiro I, Mufti GJ, Thomas NS, et al. Direct transcriptional regulation of Bim by FoxO3a mediates STI571-induced apoptosis in Bcr-Abl-expressing cells. Oncogene 2005;24:2317–29.
33. Busuttil V, Droin N, McCormick L, Bernassola F, Candi E, Melino G, et al. NF-kappaB inhibits T-cell activation-induced, p73-dependent cell death by induction of MDM2. Proc Natl Acad Sci U S A 2010;107:18061–6.
34. Brunet A, Park J, Tran H, Hu LS, Hemmings BA, Greenberg ME. Protein kinase SGK mediates survival signals by phosphorylating the forkhead transcription factor FKHRL1 (FOXO3a). Mol Cell Biol 2001;21:952–65.
35. Obsil T, Obsilova V. Structure/function relationships underlying regulation of FOXO transcription factors. Oncogene 2008;27:2263–75.
36. Modur V, Nagarajan R, Evers BM, Milbrandt J. FOXO proteins regulate tumor necrosis factor-related apoptosis inducing ligand expression. Implications for PTEN mutation in prostate cancer. J Biol Chem 2002;277:47928–37.
37. Wang F, Marshall CB, Yamamoto K, Li GY, Gasmi-Seabrook GM, Okada H, et al. Structures of KIX domain of CBP in complex with two FOXO3a transactivation domains reveal promiscuity and plasticity in coactivator recruitment. Proc Natl Acad Sci U S A 2012;109:6078–83.
38. Clerc I, Polakowski N, Andre-Arpin C, Cook P, Barbeau B, Mesnard JM, et al. An interaction between the human T cell leukemia virus type 1 basic leucine zipper factor (HBZ) and the KIX domain of p300/CBP contributes to the down-regulation of tax-dependent viral transcription by HBZ. J Biol Chem 2008;283:23903–13.
39. Tsai KL, Sun YJ, Huang CY, Yang JY, Hung MC, Hsiao CD. Crystal structure of the human FOXO3a-DBD/DNA complex suggests the effects of post-translational modification. Nucleic Acids Res 2007;35:6984–94.
40. Bouillet P, Zhang LC, Huang DC, Webb GC, Bottema CD, Shore P, et al. Gene structure alternative splicing, and chromosomal localization of pro-apoptotic Bcl-2 relative Bim. Mamm Genome 2001;12:163–8.
41. Gilley J, Ham J. Evidence for increased complexity in the regulation of Bim expression in sympathetic neurons: involvement of novel transcriptional and translational mechanisms. DNA Cell Biol 2005;24:563–73.
42. Gilley J, Coffer PJ, Ham J. FOXO transcription factors directly activate bim gene expression and promote apoptosis in sympathetic neurons. J Cell Biol 2003;162:613–22.
43. Marks P, Rifkind RA, Richon VM, Breslow R, Miller T, Kelly WK. Histone deacetylases and cancer: causes and therapies. Nat Rev Cancer 2001;1:194–202.
44. Fullgrabe J, Kavanagh E, Joseph B. Histone onco-modifications. Oncogene 2011;30:3391–403.
45. Wang F, Marshall CB, Li GY, Yamamoto K, Mak TW, Ikura M. Synergistic interplay between promoter recognition and CBP/p300 coactivator recruitment by FOXO3a. ACS Chem Biol 2009;4:1017–27.
46. Egle A, Harris AW, Bouillet P, Cory S. Bim is a suppressor of Myc-induced mouse B cell leukemia. Proc Natl Acad Sci U S A 2004;101:6164–9.
47. Paschos K, Smith P, Anderton E, Middeldorp JM, White RE, Allday MJ. Epstein-barr virus latency in B cells leads to epigenetic repression and CpG methylation of the tumour suppressor gene Bim. PLoS Pathog 2009;5:e1000492.
48. Hu MC, Lee DF, Xia W, Golfman LS, Ou-Yang F, Yang JY, et al. IkappaB kinase promotes tumorigenesis through inhibition of forkhead FOXO3a. Cell 2004;117:225–37.

Arch Virol (2014) 159:1849–1856
DOI 10.1007/s00705-014-2099-y

BRIEF REPORT

Development of T cell lymphoma in HTLV-1 bZIP factor and Tax double transgenic mice

Tiejun Zhao · Yorifumi Satou · Masao Matsuoka

Received: 13 January 2014 / Accepted: 22 April 2014 / Published online: 13 May 2014

Abstract Adult T-cell leukemia (ATL) is an aggressive T-cell malignancy caused by human T-cell leukemia virus type 1 (HTLV-1). ATL cells possess a CD4+ CD25+ phenotype, similar to that of regulatory T cells (Tregs). Tax has been reported to play a crucial role in the leukemogenesis of HTLV-1. The HTLV-1 bZIP factor (HBZ), which is encoded by the minus strand of the viral genomic RNA, is expressed in all ATL cases and induces neoplastic and inflammatory disease *in vivo*. To test whether HBZ and Tax are both required for T cell malignancy, we generated HBZ/Tax double transgenic mice in which HBZ and Tax are expressed exclusively in CD4+ T cells. Survival was much reduced in HBZ/Tax double-transgenic mice compared with wild type littermates. Transgenic expression of HBZ and Tax induced skin lesions and T-cell lymphoma in mice, resembling diseases observed in HTLV-1 infected individuals. However, Tax single transgenic mice did not develop major health problems. In addition, memory CD4+ T cells and Foxp3+ Treg cells counts were increased in HBZ/Tax double transgenic mice, and their proliferation was enhanced. There was very little difference between HBZ single and HBZ/Tax double transgenic mice. Taken together, these results show that HBZ, in addition to Tax, plays a critical role in T-cell lymphoma arising from HTLV-1 infection.

Keywords HTLV-1 · HBZ · Tax · Transgenic mice · Lymphoma

Electronic supplementary material The online version of this article (doi:10.1007/s00705-014-2099-y) contains supplementary material, which is available to authorized users.

T. Zhao (✉)
College of Chemistry and Life Sciences, Zhejiang Normal University, 688 Yingbin Road, Jinhua 321004, Zhejiang, China
e-mail: tjzhao@zjnu.cn

T. Zhao · Y. Satou · M. Matsuoka
Laboratory of Virus Control, Institute for Virus Research, Kyoto University, Kyoto, Japan

Present Address:
Y. Satou
Priority Organization for Innovation and Excellence, Center for AIDS Research, Kumamoto University, Kumamoto, Japan

Introduction

Human T-cell leukemia virus type1 (HTLV-1) was the first retrovirus proven to be associated with human disease. Infection with HTLV-1 causes adult T-cell leukemia (ATL) [20, 24]. ATL cells possess a CD4+ CD25+ phenotype, similar to that of regulatory T cells (Tregs). Previous report showed that HTLV-1 provirus is detected mainly in CD4+ memory T cells and Treg cells, suggesting that HTLV-1 favors Treg cells and memory T cells *in vivo* [10, 23, 26].

HTLV-1 encodes several regulatory (*tax* and *rex*) and accessory (*p12*, *p13*, and *p30*) genes in the pX region between the *env* gene and the 3′ Long terminal repeat (LTR) [19]. Another gene, the *HTLV-1 bZIP factor* (*HBZ*), is encoded by the minus strand of the HTLV-1 genome [4]. Among the proteins encoded by these genes, Tax and HBZ play critical roles in ATL [5, 16]. Accumulating evidence shows that Tax can immortalize human primary T cells, enhance viral replication and support cellular proliferation [5]. However, the expression of Tax cannot be detected in approximately 60 % of fresh ATL cells because of genetic and epigenetic changes in the HTLV-1 provirus, which indicated that Tax may not be essential for the development of ATL [15]. We reported previously that HBZ is

consistently expressed in all ATL cells and promotes proliferation of ATL cells [21]. Non-sense mutations of all HTLV-1 genes except HBZ were generated by APOBEC3G (A3G), suggesting that HBZ is indispensable for the growth and survival of HTLV-1 infected cells [3].

It is noteworthy that Tax and HBZ synergistically regulated the viral transcription and cellular signaling pathways in ATL [29]. HBZ suppressed Tax-mediated HTLV-1 viral transcription through interaction with cAMP response element-binding protein (CREB) [12]. Additionally, HBZ selectively inhibited the classical nuclear factor-κB (NF-κB) pathway which was activated by Tax [27]. We reported that HBZ induced the differentiation of Treg cells by activating the transforming growth factor-β (TGF-β) pathway [28]. Contrariwise, three distinct mechanisms by which Tax suppressed TGF-β–mediated signaling were reported [1, 11, 17]. Taken together, we speculated that the complementary effect of Tax and HBZ on regulating signaling pathways may facilitate better survival of HTLV-1 infected cells and help the cancer cells escape immune attack.

To test the effect of synchronous expression of HBZ and Tax on T cell malignancy in vivo, we generated double transgenic mice expressing HBZ and Tax under the control of the CD4 promoter. In the present study, we found that HBZ/Tax mice have increased memory CD4+ T cells and Foxp3+ Treg cells, resulting in the development of skin lesions and T-cell lymphoma. Both the skin lesions and the lymphoma resemble diseases observed in HTLV-1 infected individuals.

Material and methods

Mice and cell cultures

C57BL/6 J mice were purchased from CLEA Japan. Transgenic HBZ mice expressing HBZ specifically in CD4+ cells have been described elsewhere [22, 25]. Tax single transgenic mice were generated as previously reported [22]. Male HBZ transgenic mice were mated with female Tax transgenic mice, and offspring were typed for the presence of each transgene. Wild-type, HBZ, and Tax single transgenic mice were maintained as controls along with experimental HBZ/Tax transgenic offspring.

All animal experimentation was performed in strict accordance with the Japanese animal welfare bodies, and the Regulation on Animal Experimentation at Kyoto University. The protocol was approved by the Institutional Animal Research Committees of Kyoto University and Zhejiang Normal University. All efforts were made to minimize suffering.

ATL cell lines, ATL-43T and MT-1, were cultured in RPMI-1640 containing 10 % FBS and antibiotics. 293FT cells were maintained as described previously [27].

Semiquantitative RT-PCR and real-time PCR

Total RNA was isolated using Trizol Reagent (Invitrogen) according to the manufacturer's instructions. We reverse-transcribed total RNA into single-stranded cDNA with SuperScript III reverse transcriptase (Invitrogen). For semiquantitative PCR, cDNA was amplified by increasing PCR cycles using forward (F) and reverse (R) primers specific to the target genes. The expression of transgenic genes was quantified by real-time PCR using the Taqman Universal PCR Master Mix (PE Applied Biosystems) according to the manufacturer's instructions.

Lentiviral vector construction and transfection of recombinant lentivirus

We cloned Tax cDNA into a lentiviral vector, pCSII-EF-MCS. Recombinant lentivirus was produced as described. ATL-43T cells were incubated with concentrated vector stocks in the presence of 4 μg/mL polybrene.

Cell isolation and flow cytometric analysis

Murine spleen was carefully crushed to release the lymphocytes. Splenic erythrocytes were eliminated with NH_4Cl. Cells were washed with PBS containing 1 % FBS. After centrifugation, cells were incubated with antibodies for 30 min at 4 °C, and then analyzed with a flow cytometer (BD FACSCanto II, BD Biosciences). For intracellular staining, we used a mouse Foxp3 staining kit according to its protocol (eBioscience).

BrdU staining

In vivo proliferation was measured by BrdU incorporation. BrdU (Nacalai Tesque) was dissolved in PBS (3 μg/ml), and then 200 μl was injected intraperitoneally into transgenic and non-transgenic mice twice a day for three days. BrdU incorporation in CD4+ splenocytes was detected using FITC BrdU Flow Kits (BD Pharmingen) according to the manufacturer's instructions.

Statistical analysis

Statistical analyses were performed using the unpaired student *t* test.

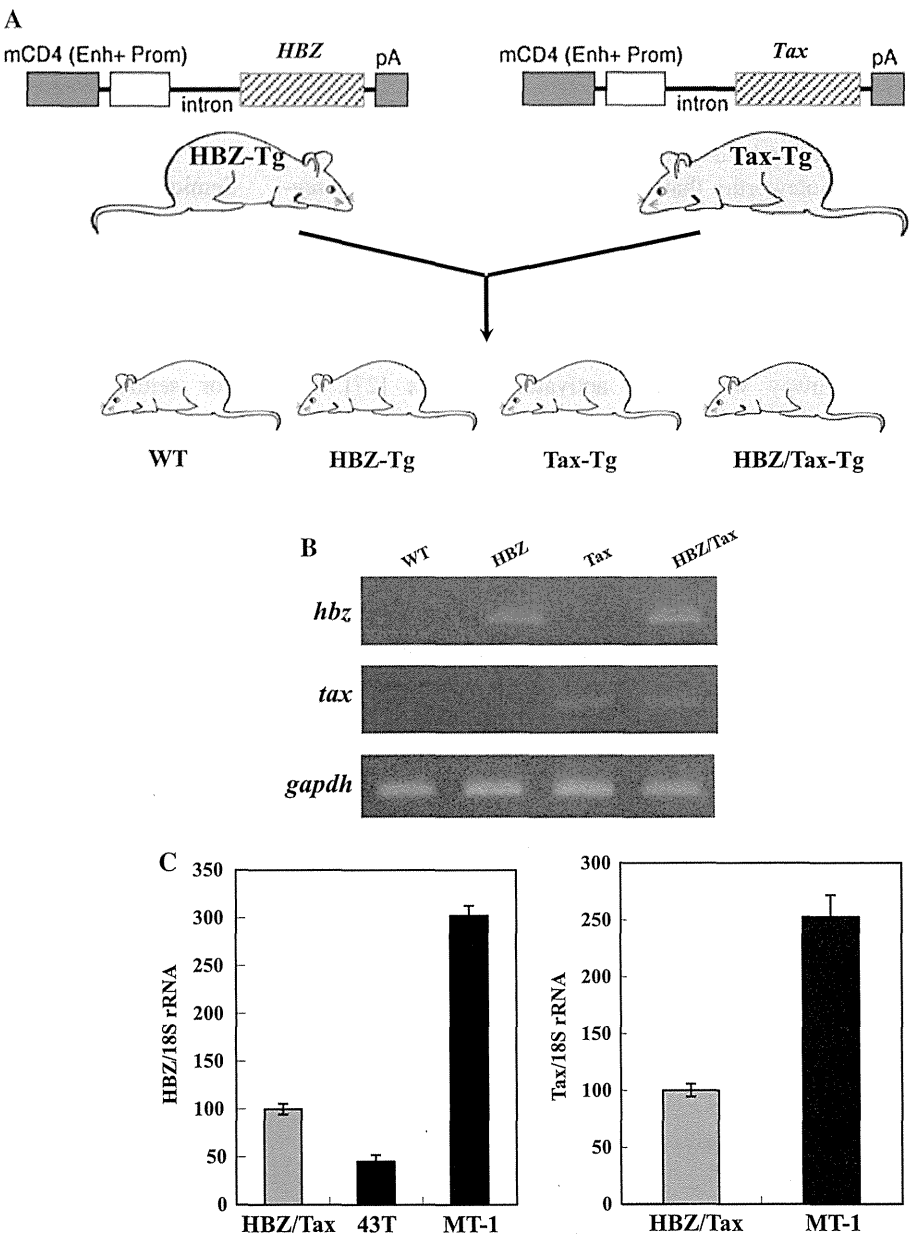

Fig. 1 Generation of HBZ/Tax transgenic (Tg) mice. (A) Schematic representation of the HBZ and Tax transgene. The promoter (Prom) and enhancer (Enh) of the mouse CD4 (mCD4) gene were ligated to HBZ and Tax cDNA plus the polyadenylation signal sequence of SV40. (B) Expression of HBZ and Tax transcripts was detected by RT-PCR in purified CD4+ splenocytes from transgenic mice. (C) Transcripts of the HBZ and Tax genes in CD4+ splenocyte from HBZ/Tax-transgenic mice or ATL cell lines were quantified by real time PCR. ATL-43T and MT-1 are derived from ATL cells

Results

In the development of ATL, Tax is thought to play critical role in leukemogenesis because of its pleiotropic functions [5]. HBZ was constitutively expressed in all ATL cases, and involved in cell proliferation [21]. Additionally, HBZ modulated Tax-mediated viral gene transcription and cellular signaling, suggesting that HBZ cooperates closely with Tax in ATL [2, 7, 12–14, 27, 28]. However, the relevance to T cell malignancy of combined up-regulation of Tax and HBZ has not been established. Since HTLV-1 mainly infects CD4+ T cells, we generated transgenic mice expressing HBZ and Tax under the control of the murine CD4-specific promoter/enhancer/silencer. To test whether HBZ and Tax could cooperate in the development of T cell malignancies, we took advantage of the availability of HBZ and Tax transgenic mice and produced double-transgenic mice expressing both HBZ and Tax in T lymphocytes (Fig. 1A). As shown in Fig. 1B, HBZ and Tax transgene expression was detected by RT-PCR by using CD4+ splenocytes from age-matched mice of the different genotypes. Moreover, HBZ did not interfere with the expression of Tax in double transgenic mice. As shown in Figure 1C, the expression level of HBZ and Tax in transgenic mice was similar to that of ATL cell lines.

Tax single transgenic mice did not develop major health problems, and had a normal life span, as shown in Fig. 2A. In contrast, survival of HBZ and HBZ/Tax double

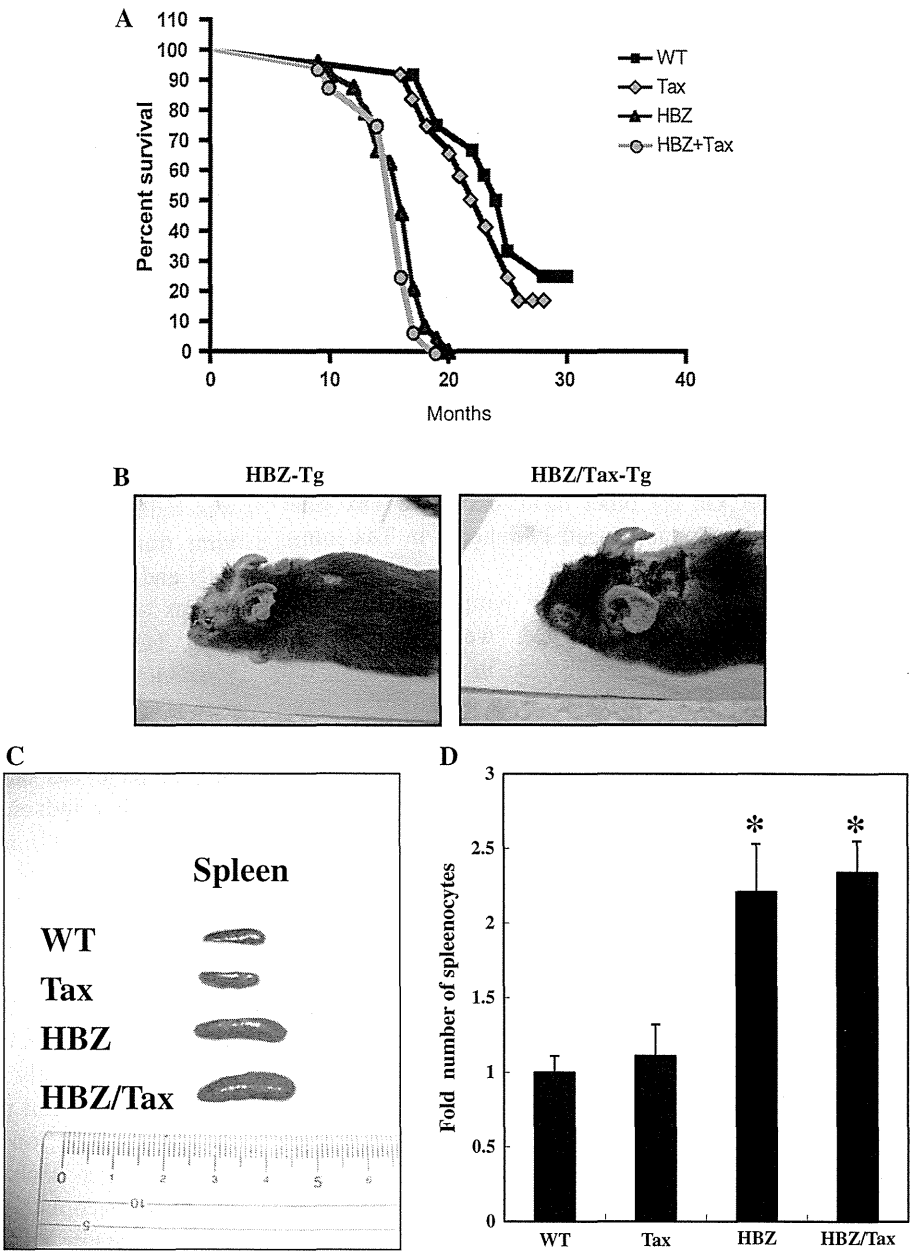

Fig. 2 Characterization of transgenic mice. (A) Kaplan–Meier analysis of survival of wild-type, HBZ single-, Tax single-, and HBZ/Tax double transgenic mice. (B) An HBZ-transgenic and HBZ/Tax mouse with typical skin symptom. (C) Representative examples of spleens from age-matched transgenic mice. (D) Total number of splenocytes of transgenic mice are compared.*, $P < 0.05$ when transgenic mice are compared with wild type littermates by unpaired t test

transgenic mice was much reduced. Some of these mice died as early as ten months after birth. By 20 months, <5% of the HBZ and HBZ/Tax mice remained alive. Interestingly, there is not much difference in survival time between HBZ single transgenic mice and HBZ/Tax double transgenic mice.

Consistent with previous reports, HBZ transgenic mice developed skin lesions by 4 months of age, non-transgenic littermates developed no disease. As shown in Fig. 2B, HBZ/Tax double transgenic mice had similar skin symptoms as HBZ transgenic mice. In Tax transgenic mice, we did not observe inflammatory lesions in the skin (data not shown). Analysis of spleen size in transgenic mice expressing HBZ or Tax alone or in combination revealed splenomegaly in HBZ and HBZ/Tax lines, while tax transgenic mice present spleens of normal size. Moreover, age-matched HBZ/Tax double-transgenic mice had spleens similar in size and weight to HBZ single transgenic mice. Representative examples of the spleens from the various transgenic mice are shown in Fig. 2C. Next, we analyzed the total number of splenic CD4+ T cells in each transgenic line. As shown in Fig. 2D, HBZ and HBZ/Tax mice had, on average, twice the CD4+ splenocytes of wild-type littermates, whereas Tax mice had equal numbers of splenocytes as non-transgenic mice.

Table 1 The incidence of lymphoma in transgenic mice

	WT	Tax-Tg	HBZ-Tg	HBZ/Tax-Tg
Total	52	42	43	32
Lymphoma	2.7 %	2.2 %	32.2 %	34.7 %

The total number of mice and percentage of transgenic mice with lymphoma are listed

Analogous to the incidence of ATL in humans, 32.2 % of HBZ transgenic mice developed T-cell lymphomas after 14 months, in contrast with 2.7 % of non-transgenic mice. As shown in Table 1, the incidence of T-cell lymphomas in HBZ/Tax double transgenic mice is similar to that in HBZ transgenic mice. On the other hand, excessive Tax gene expression did not induce T-cell lymphoma in Tax transgenic mice.

To study the cellular basis of lymphomagenesis in HBZ/Tax double transgenic mice, we next analyzed the phenotype and FoxP3 expression in three month old mice before they developed pathological manifestations. A previous report showed that effector/memory and CD4+ FoxP3+ regulatory T cells were increased in the HBZ-transgenic mice [22]. We found in this study that the percentage of CD4 single positive T cells increased in the HBZ/Tax transgenic mice (Fig. 3). Moreover, transgenic expression of Tax and HBZ induced Foxp3 expression. We also observed an increased population of effector/memory T cells in the HBZ/Tax transgenic mice, yet the percentage of effector/memory T cells or Treg cells in the Tax-transgenic mice did not change significantly. In addition, there is not much difference in the enhancement of memory and FoxP3+ CD4+ regulatory T-cell populations between HBZ and HBZ/Tax transgenic mice. Taken together, these observations demonstrate that HBZ increased memory T cells and Foxp3 induction in CD4+ T cells regardless of Tax.

We further studied whether Tax has any influence on the generation of Foxp3+ T cells *in vivo*. As shown in Supplemental Fig. 1, retrovirally expressed Tax protein could not increase the level of Foxp3 in ATL-43T, an HTLV-1-associated cell line, which does not express Foxp3.

To study the growth-promoting activity of the HBZ and Tax genes, we assessed the proliferation of CD4+ T cells in transgenic mice by incorporation of BrdU. We found that, in HBZ and HBZ/Tax transgenic mice, the proliferation of CD4+ T cells was three fold-higher than in non-transgenic mice, whereas the proliferation of CD4+ T cells of Tax transgenic mice was similar to that in non-transgenic mice (Fig. 4).

All of these results suggest an important role for HBZ, in addition to Tax, in the oncogenic activity of HTLV-1.

Discussion

Over the past 35 years, substantial effort has been made toward investigating the HTLV-1 associated viral proteins and their regulatory functions [15]. Tax has been shown to be a viral oncogene, since it transforms and immortalizes rodent cells and human T-lymphocytes [15]. HBZ is the only viral gene which is conserved and expressed in all ATL cases, indicating that HBZ is indispensable for HTLV-1 infection and development of ATL [16]. Accumulating evidences shows that HBZ and Tax synergistically dysregulate cell signaling pathways in ATL and determine the cell fate, despite the fact that HBZ and Tax have opposite effects on regulation of cellular activity [2, 13, 14, 27, 28]. For example, HBZ was found to inhibit the Tax-mediated transactivation of viral transcription from the 5′LTR by interacting with JUN and CREB. HBZ overcame the suppression function of Tax on the TGF-β pathway, leading to the activation of TGF-β signaling and differentiation of Foxp3+ CD4+ regulatory T cells. Thus, we proposed that HTLV-1 may take advantage of the complementary functions of HBZ and Tax to facilitate the onset of ATL. So far, there has been no direct evidence for HBZ and Tax together inducing T cell malignancy in vivo. The present study demonstrated that HBZ/Tax double transgenic mice indeed developed T cell lymphoma and inflammation via increased memory T cells and Treg cells.

Since Tax is the major target of cytotoxic T-lymphocytes (CTLs), host cells have developed several mechanisms to silence the expression of Tax [9]. Tax transcripts are detected in only ~40 % of ATL patients. Therefore, HBZ maintains cell proliferation in the late stage of ATL when Tax expression is lost. In this study, we demonstrated that HBZ/Tax double and HBZ single transgenic mice developed neoplastic and inflammatory diseases, while mice expressing only Tax did not. Thus, we suggest that constitutively expressed HBZ is the predominant driver of leukemogenesis of ATL.

It has been reported that Tax transgenic mice develop tumors [6, 8, 18]. In those reports, the type of tumor induced by Tax depended on the promoter used. In this study, we generated Tax transgenic mice using the CD4-specific promoter/enhancer/silencer which has previously been used in generating HBZ-transgenic mice. The Tax transgenic mice thus generated did not show any change in the number of Foxp3+ Treg cells or memory T cells, in contrast to mice expressing HBZ, who developed T cell lymphomas. Moreover, since there was no difference in disease between HBZ single and HBZ/Tax double transgenic mice, expression of Tax did not synergistically enhance the lymphomagenesis by HBZ. These data

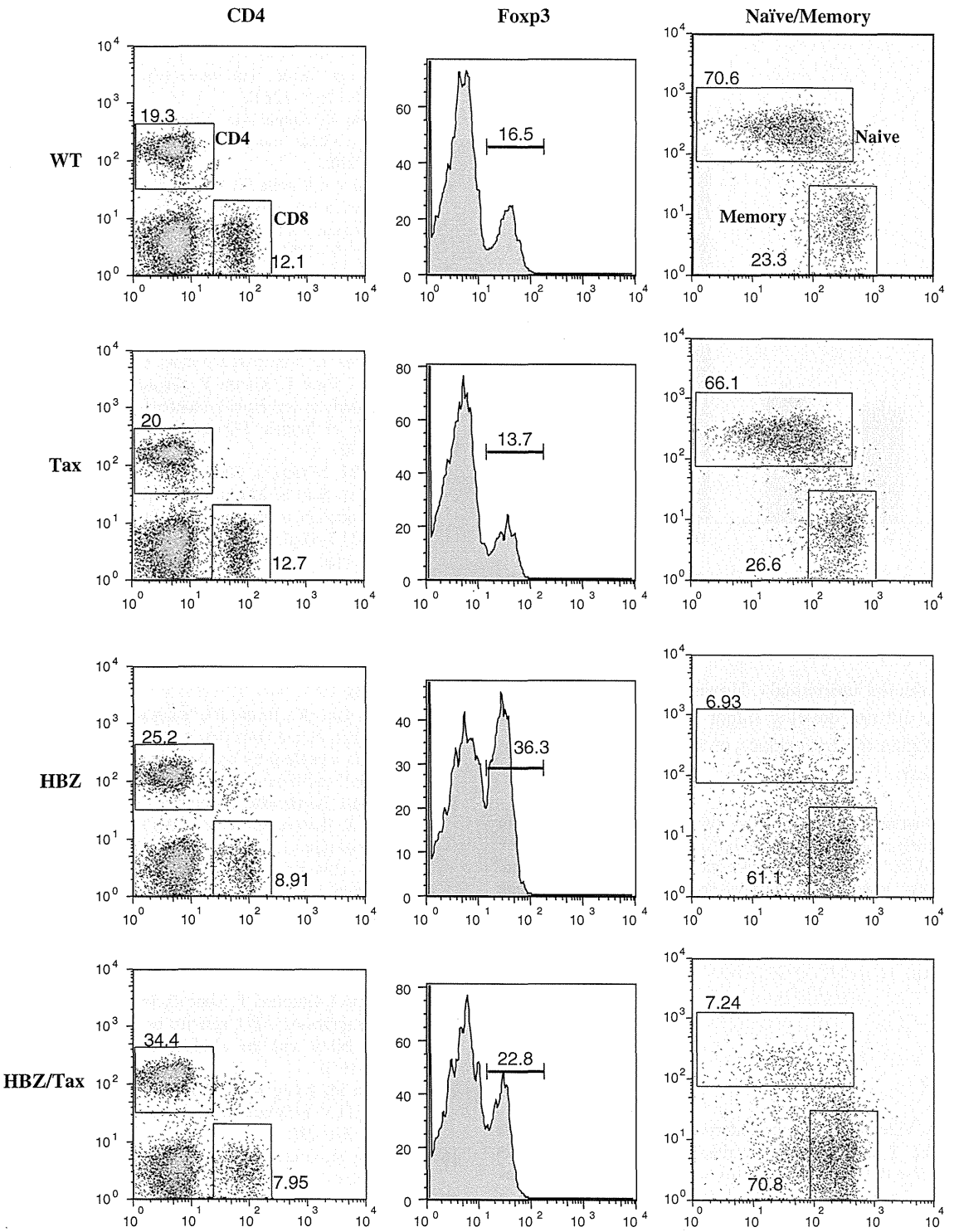

Fig. 3 Transgenic expression of HBZ/Tax in CD4+ T cells increases Foxp3+ Treg and memory T cells. Mouse splenocytes were stained with the indicated antibodies, and analyzed by flow cytometry. Representative dot plots gated on the CD4+ population are shown. For these experiments, HBZ and HBZ/Tax transgenic mice without any symptoms were used

suggest that HBZ, rather than Tax, is responsible for conferring the specific phenotype of HTLV-1 infected cells, and for triggering the development of ATL.

In conclusion, we showed that HBZ single and HBZ/Tax double transgenic mice spontaneously develop T cell lymphomas and inflammatory diseases similar to those in